TECHNISCHE UNIVERSITÄT MÜNCHEN

Lehrstuhl für Humanbiologie

Identification and functional analysis of the Membrane Binding Domain of Helicobacter pylori protein CagA

Christiane Pelz

Vollständiger Abdruck der von der Fakultät Wissenschaftszentrum Weihenstephan für Ernährung, Landnutzung und Umwelt der Technischen Universität München zur Erlangung des akademischen Grades eines

Doktors der Naturwissenschaften

genehmigten Dissertation.

Vorsitzender:		Univ.-Prof. Dr. D. Haller
Prüfer der Dissertation:	1.	Univ.-Prof. Dr. M. Schemann
	2.	Univ.-Prof. Dr. R. Schmid

Die Dissertation wurde am 28.04.2010 bei der Technischen Universität München eingereicht und durch die Fakultät Wissenschaftszentrum Weihenstephan für Ernährung, Landnutzung und Umwelt am 09.09.2010 angenommen.

Table of contents

Table of Figures

Abbreviations

3D	3 Dimensional
Arg	ABL-related gene
APC/GSK3	Adenomatous Polyposis Coli/Glycogen Synthase Kinase
AA	Amino Acid
APS	Ammonium Persulphate
ANOVA	Analysis of Variances
AJC	Apical Junctional Complex
ECM	Cell-Extracellular Matrix
c-Abl	Cellular Abelson murine leukemia viral oncogene homolog
cm	Centimetre
CRPIA	Conserved Repeat Responsible for Phosphorylation
CagA	Cytotoxin-associated gene A
°C	Degree Celsius
DAPI	4', 6-Diamidin-2'-phenylindol-dihydrochlorid
DNA	Deoxyribonucleic acid
DMSO	Dimethyl sulfoxide
DTT	DL-Dithiothreitol
dox	Doxycycline
DMEM	Dulbecco's Modified Eagle Medium
EMT	Epithelial-Mesenchymal Transition
EDTA	Ethylenediaminetetraacetic acid
Erk	Extracellular-signal-regulated kinase
FBS	Fetal Bovine Serum
FAK	Focal Adhesion Kinase
EPISA	Glucin - Prolin - Isoleucin - Serin - Alanin
EPIYA	Glucin - Prolin - Isoleucin - Tyrosin - Alanin
GP135	Glycoprotein 135
g	Gram
GFP	Green Fluorescent Protein
H. pylori	Helicobacter pylori
h	Hours
IB	Immunoblot
IF	Immunofluorescence
Kb	Kilo base

kDa	Kilo Dalton
l	Litre
LB	Luria broth
LEF	Lymphoid Enhancer Factor
MDCK	Madine Darby Canine Kidney
MBD	Membrane Binding Domain
µg	Microgram
µl	Microlitre
µm	Micrometer
µM	Micromolar
MARK	Microtubule affinity-regulating kinase
mg	Milligram
ml	Millilitre
mm	Millimetre
mM	Millimolar
M	Molar
CM	Multimerisation Sequence
TEMED	N, N, N', N'-tetramethylethylenediamine
ng	Nanogram
nm	Nanometre
nM	Nanomolar
NFκB	Nuclear factor kappa B
OD	Optical Density
PAR	Partitioning-defective
PBS	Phosphate Buffered Saline
PCR	Polymerase Chain Reaction
RFP	Red Fluorescent Protein
rfc	Relative centrifugal force
sec	Seconds
SDS	Sodium Dodecyl Sulfate
SFKs	Src family kinases
SD	Standard deviation
SEM	Standard error of means
SBP/CBP	Streptavidin Binding Protein Calmodulin Binding Protein
TCF	T-cell factor
tetO	Tet operator sequence

tet	Tetracycline
TRE	Tetracycline response element
TER	Transepithelial Electrical Resistance
TFSS	Type IV secretion system
UV	Ultraviolet
wt	Wild type
ZO	Zonula Occludens

1 Introduction

1.1 Helicobacter pylori infection and gastric cancer

Helicobacter pylori (*H. pylori*) infection is one of the most common bacterial infections worldwide. The infection rate varies from 10%-40% in western countries up to 90% in developing countries. The *H. pylori* infection is acquired mostly throughout childhood and persists lifelong (Pounder and Ng, 1995).

H. pylori is a spiral shaped bacterium, which was first described by Marshall and Warren in 1984. It is a microaerophilic gram-negative bacterium, with 2 to 6 flagella, which confer motility and allow rapid movement in viscous solutions such as the mucus layer overlying the gastric epithelial cells (O'Toole et al., 2000). Marshall and Warren found that the bacteria were present in almost all patients with active chronic gastritis, duodenal ulcer, or gastric ulcer and concluded that it may be an important factor in the aetiology of these diseases (Marshall and Warren, 1984).

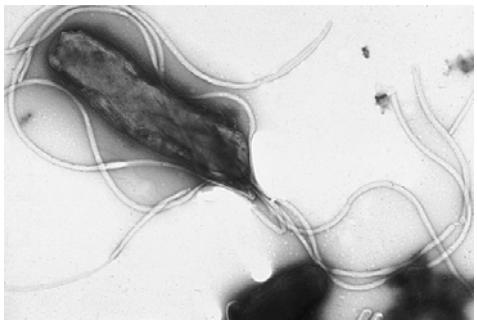

Figure 1: *H. pylori*. Electron micrograph of *H. pylori* possessing multiple flagella (negative staining). (Yutaka Tsutsumi)

The colonisation with *H. pylori* is not a disease by itself, but it is a risk factor for developing various clinical disorders of the upper gastrointestinal tract. Gastric colonisation is often accompanied by development of acute gastritis. About 10%-20% percent develop gastric or duodenal ulcers and approximately 1-2% develop gastric lymphoma or gastric cancer (Ernst et al., 2000; Kuipers et al., 1995). Furthermore epidemiological data suggest that 60% to 90% of all gastric cancer is attributed to *H. pylori* infection (Malfertheiner et al., 2005; Uemura et al., 2001), hence infection with *H. pylori* is a high risk factor for developing gastric cancer.

H. pylori can be divided in two subclasses, cytotoxin-associated gene A (CagA) positive and CagA negative *H. pylori* strains. CagA positive strains can be further subdivided into Western and Eastern strains meaning that CagA was isolated from patients of Western countries or patients of East Asian countries, respectively. There is evidence that CagA from East Asian isolates is more potent in inducing host cell responses (Higashi et al., 2002a; Naito et al., 2006).

The relative risk for gastric cancer is higher when patients are infected with CagA positive *H. pylori* strains compared to CagA negative strains (Blaser et al., 1995; Brenner et al., 2004), suggesting that CagA is a virulence factor for developing gastric cancer. Studies in animal models further support the idea. Data from transgenic expression of CagA in a mouse model suggest that CagA causes the formation of gastric neoplasms independent of chronic *H. pylori* infection (Ohnishi et al., 2008). In Mongolian gerbils CagA positive *H. pylori*, but not a *H. pylori* mutant strain lacking CagA, caused early immunological responses, which eventually led to precancerous gastric changes (Wiedemann et al., 2009).

1.2 The CagA protein and its different functional domains

Much of the research into Helicobacter has strongly focused on *H. pylori* protein CagA. It is the only *H. pylori* protein, which is known to be injected into the epithelial cells of the gastric mucosa.

The *CagA* gene is part of a 40 kilobase DNA Fragment known as the cag pathogenicity island, a set of genomic DNA inserted into the *H. pylori* genome encoding a type IV secretion system (TFSS). *H. pylori* attaches to epithelial cells where it forms the TFSS, a needle like structure through which the CagA protein is injected into the host cell. Upon delivery, the CagA protein localises to the plasma membrane where it is tyrosin-phosphorylated at the C-terminal amino acid motif Glucin - Prolin - Isoleucin - Tyrosin - Alanin (EPIYA) via Src family kinases and c-Abl kinases (Asahi et al., 2000; Odenbreit et al., 2000; Poppe et al., 2007; Selbach et al., 2002; Stein et al., 2002; Tammer et al., 2007).

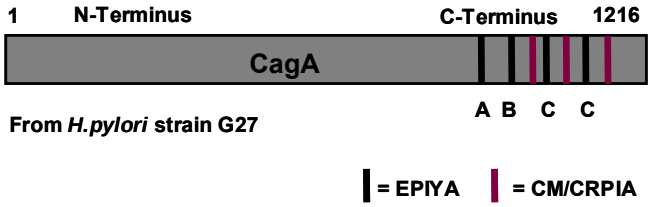

Figure 2: CagA from H. pylori strain G27.
Schematic drawing.

The EPIYA motif is a conserved amino acid sequence which has several repeats. The first and second EPIYA sequences are termed A and B motif and are present in almost all sequenced *H. pylori* strains. Western CagA consists of EPIYA A B and up to three EPIYA C motifs. The EPIYA C motifs are formed by a duplication of a 34 amino acid stretch containing an EPIYA motif. In contrast, East Asian CagA has a specific EPIYA D motif, which is highly homologous to Western specific EPIYA C motif (Higashi et al., 2002a). The G27 *H. pylori* strain used in this work has four EPIYA repeats: EPIYA ABCC (Figure 2).

Additionally to the EPIYA motif, there is a second specific sequence in the C-terminus of CagA, the multimerisation sequence (CM) also named CRPIA motif (conserved repeat responsible for phosphorylation) (Ren et al., 2006; Suzuki et al., 2009). The CM/CRPIA motif is a conserved sequence present in multiple repeats in Western CagA and one repeat in Eastern CagA. It was identified as a 16 amino acid stretch, which mediates multimerisation of CagA (Ren et al., 2006).

Most Eastern CagA strains consist of only one CM/CRPIA sequence (amino acid code FPLRRSAAVNDLSKVG) whereas Western CagA strains often consist of at least two CM/CRPIA sequences. The CagA from *H. pylori* strain G27 contains three CM/CRPIA sequences with the amino acid code FPLKRHDKVDDLSKVG, one before the first EPIYA C segment and one after each EPIYA C segment (Figure 2).

After the injection of CagA into the epithelial host, CagA is localised to the membrane of the epithelial cells. Interestingly, published data regarding the CagA interaction with the epithelial membrane are inconsistent with one another. Higashi et al. described that EPIYA motifs mediate membrane attachment of CagA, showing that a CagA mutant lacking the N-terminus is localised to the membrane whereas a mutant lacking the C-terminus containing the EPIYA motif was detected in the cytoplasm (Higashi et al., 2005). In contrast, Bagnoli et al. demonstrated that the N-terminus of CagA directs the protein to the plasma membrane of epithelial cells independent of EPIYA motifs (Bagnoli et al., 2005). In their hands, a CagA mutant lacking the N-terminus, but containing the EPIYA motifs in the C-terminus of CagA is distributed in the cytoplasm. At first glance these results seem to contradict each other. That raised the question if CagA has two distinct binding domains to interact with epithelial plasma membranes and if this affects host cell signalling hence phenotypic response.

After membrane localisation CagA is phosphorylated first by Src family kinases (SFKs), which control cytoskeletal processes, cell proliferation and differentiation in normal cells, but are also key players in carcinogenesis (Selbach et al., 2002; Stein et al., 2002). Then Src kinases are inactivated and Abl kinases (c-Abl and Arg) are activated and continuously phosphorylate CagA (Poppe et al., 2007; Tammer et al., 2007). Phosphorylation of CagA is a highly dynamic process and there is evidence that not all EPIYA motifs within CagA are phosphorylated (Backert et al., 2001).

Half-life of CagA is very short (Ishikawa et al., 2009). Upon delivery into host cells and phosphorylation, the mean half-life of CagA is 148 minutes and 200 minutes for transfected CagA, respectively. This half-life is independent of EPIYA

phosphorylation, but for a deletion mutant missing the CM/CRPIA sequence, the half-life of CagA is significantly reduced, suggesting that the interaction of CagA with Par1 increases CagA stability (see 1.3).

1.3 Role of CagA protein in cancer formation

Within the host cell CagA interacts with various intracellular proteins like SHP-2, ZO-1 or Par1b and also interferes with multiple host cell signalling pathways such as TCF/β-Catenin or NFκB signalling pathways *in vitro*. The following paragraph will elucidate the different functions.

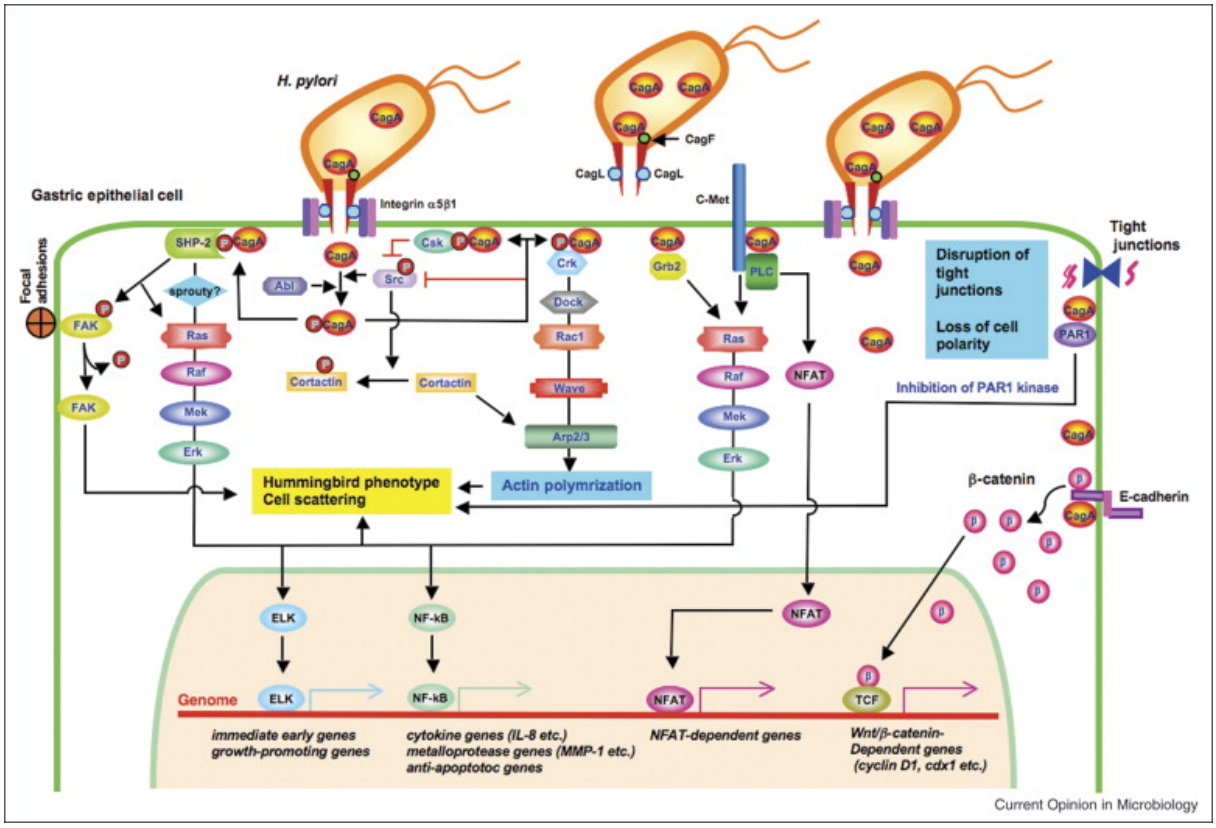

Figure 3: Overview of the CagA gastric- epithelial cell interactions. Upon delivery of CagA into gastric epithelial cells it is phosphorylated and interacts with various proteins in a tyrosine phosphorylation-dependent and independent manner leading to cell elongation, loss of cell polarity and disruption of tight junctions. CagA also binds to and inhibits PAR1 kinase to elicit junctional and polarity defects. Furthermore, CagA interacts with E-cadherin and thereby destabilizes E-cadherin/β-catenin complex to elicit deregulated Wnt/β-catenin signalling. (from Hatakeyma, 2008)

After translocation into epithelial host cells and phosphorylation at the EPIYA motifs CagA interacts with SHP-2, a protein that is involved in a variety of human malignancies (Mohi et al. 2007). The interaction of phosphorylated CagA with SHP-2 leads to activation of SHP-2 phosphatase resulting in an elongated cell phenotype also referred to as the hummingbird phenotype. Activated SHP-2 dephosphorylates

focal adhesion kinase (FAK) and inhibits kinase activity eliciting elevated cell motility by reducing active focal adhesion spots. Cells form extrusions, which are at least as long as the cell body. Important for the stable interaction with SHP-2 is the multimerisation of CagA mediated through the CM/CRPIA motif (Higashi et al., 2002b; Ren et al., 2006). CagA elongation is commonly used as a marker for functional CagA or as a marker for successfully infected cells and as readout for host cell responses regarding signalling pathways. CagA-activated SHP-2 also causes sustained Erk MAP kinase activation, which stimulates cell-cycle progression (Higashi et al., 2004). Because abnormal proliferation as well as abnormal cell motility are characteristics of transformed cells, deregulation of SHP-2 by CagA may play an important role in gastric cancer development.
Another important interaction partner of CagA is the PAR1b/MARK2 serine/ threonine kinase interaction being mediated via the CM/CRPIA motif. Par1b is a member of the partitioning-defective 1 (PAR1)/microtubule affinity-regulating kinase (MARK) family that was first isolated in Caenorhabditis elegans as a product of one of the six independent ‘partitioning-defective’ (par) genes. CagA inhibits the Par1b kinase activity and thereby leads to a disorganization of the epithelial monolayer, causing junctional and polarity defects, such as the extrusion of epithelial cells from a monolayer. Moreover, inhibition of Par1b kinase activitiy seems to be critical for the induction of the hummingbird phenotype. Saadat et al. showed that simultaneous expression of Par1b abolished the effect of the hummingbird phenotype suggesting that a CagA mediated inhibition of Par1b kinase activity is required for the elongation of cells (Saadat et al., 2007). Furthermore the deletion of the CM/CRPIA sequence in an Eastern CagA strain abolished the hummingbird phenotype (Lu et al., 2008).

There are many natural variances in the CagA gene leading to different experimental results. For example, the differences in the specific amino acid codes between Eastern and Western CagA as well as the number of CM/CRPIA motifs is critical for the affinity of CagA for Par1b, in which Eastern CagA has a higher affinity for Par1b. CagA interaction with Par1b is crucial for the interaction of CagA with SHP-2 and the induction of the hummingbird phenotype. Hence the induction of elongated cells of Western CagA is less intensive than that of Eastern CagA. Also the disruption of the epithelial barrier is less intensive in Western CagA strains (Lu et. al, 2008).

Older reports state that the phosphorylation of the EPIYA motif is critical for the induction of the Hummingbird phenotype (Higashi et al. 2002b; Bagnoli et al., 2005). In these reports, deletions that were made to obtain phosphorylation mutants were often not carefully examined for additional important sequences, which may be lost, leading to false conclusions. Also natural variations between CagA from different *H. pylori* strains may lead to different results, not only for the induction of the hummingbird phenotype but also for other CagA induced effects.

The E-cadherin/β-catenin complex plays an important role in epithelial cell-cell interaction and the maintenance of the normal architecture of epithelial tissues.
It has been described that CagA interacts with E-cadherin, which leads to destabilization of the E-cadherin/b-catenin complex resulting in the accumulation of b-catenin in the cytoplasm. In the normal state cytoplasmic b-catenin is phosphorylated by the APC/GSK3 complex and thus quickly degraded through ubiquitination in the proteasom. Upon the activation by wnt ligands, the intrinsic kinase activity of the APC complex is inhibited and stable unphosphorylated b-catenin accumulates in the cytoplasm and is translocated into the nucleus, where it binds to the N-terminus of LEF/TCF transcription factors. Mutations in the wnt signalling pathways are associated with cancer formation (Clevers et al., 2006). CagA induced accumulation of b-catenin also leads to its translocation to the nucleus and to subsequent transactivation of transcription factors (Murata-Kamiya et al. 2007). This event is phosphorylation independent and mediated by the CM/CRPIA motif (Kurashima et al., 2008; Suzuki et al., 2009).
It was also reported that CagA activates the proinflammatory transcription factor NF-κb via the Ras-MAP kinase pathway in a CagA tyrosine phosphorylation independent manner (Brandt et al., 2005). Furthermore NF-κb activation could be linked to the CM/CRPYA motif (Suzuki et al., 2009).

1.4 CagA induces changes in cell polarity of polarised epithelial cells *in vitro*

The apical junctional complex (AJC) at the tip of polarised epithelial cells regulates cell-cell adhesion between neighbouring cells, the integrity of the epithelial barrier and is also important for signalling pathways controlling cell proliferation, cell differentiation and cell polarity. The AJC consists of structural and regulatory protein sub-complexes, which interact with each other. The structural proteins are divided

into tight junctions, that form the epithelial barrier via zonula occludens (ZO), claudin and occludin proteins and into adherens junctions, which are formed by cadherin and catenin proteins (Figure 4) (Vogelmann et al., 2004).

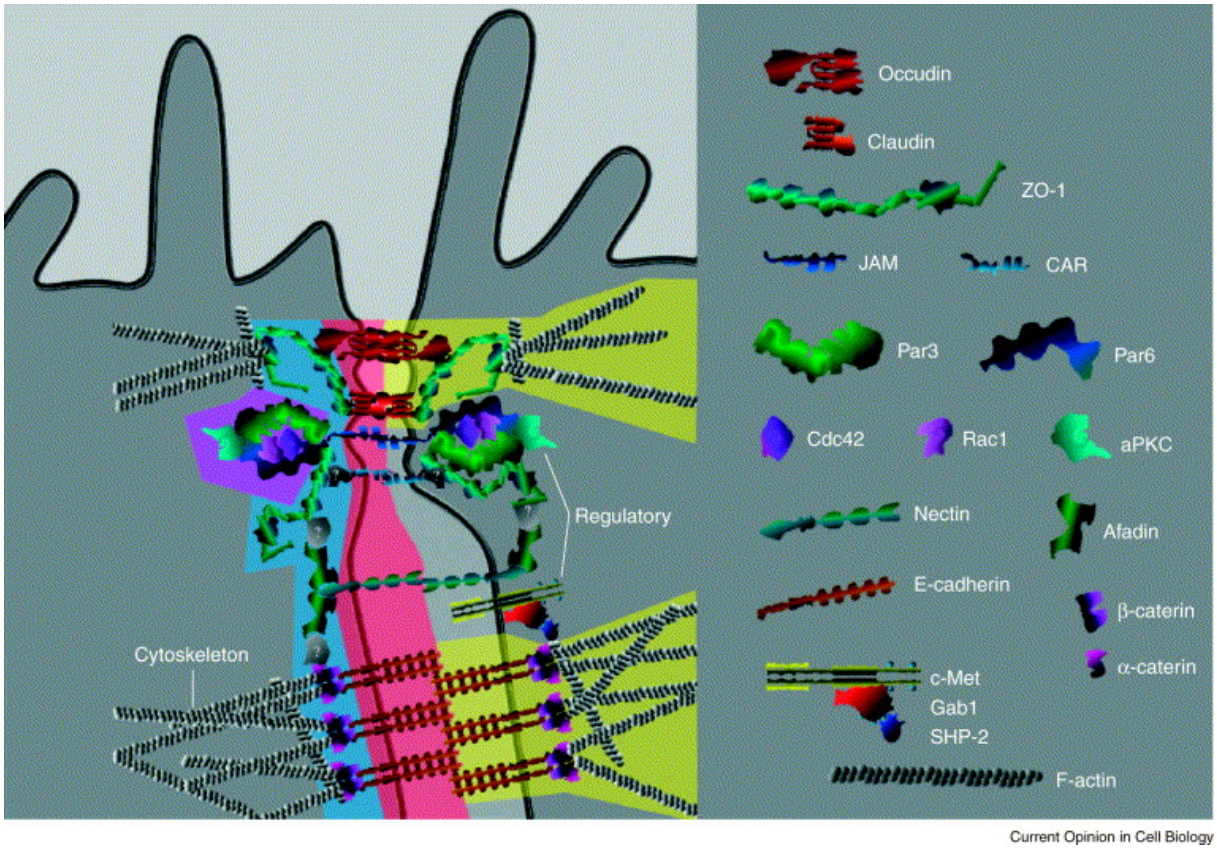

Figure 4: Model of the Apical Junctional Complex. The AJC consists of structural and regulatory protein sub-complexes. The apical junctions are divided into tight and adherens junctions. The tight junctions form the epithelial barrier via the transmembrane proteins claudins and occludin, which are linked to the actin cytoskeleton through scaffolding proteins of the ZO family. The adherens junctions are formed by E-cadherin, which is linked to the peri-junctional actin via b and a-catenins. The tight and adherens junctions interact with regulatory protein sub-complexes that are involved in the control of cell polarity, cell division, cell movement and junction assembly. (from Vogelmann et al., 2004)

It has been shown in an *in vitro* infection model that *H. pylori* attaches near the AJC to inject CagA into the host cell. The tight junction protein ZO-1 is then recruited to the sites of attachment. Upon delivery into the host cell CagA disrupts the AJC and rearranges the tight junction proteins forming a complex with JAM and ZO-1 (Amieva et al., 2003). This also leads to the disruption of the epithelial barrier resulting in an increased permeability for ions and solutes. Transgenic expression of CagA also leads to a loss of cell polarity in polarised epithelial cells resulting in mislocalisation of proteins which are confined to the apical side like GP135 or to the basolateral side like E-cadherin and to a rearrangement of ZO-1 from the AJC to the basolateral membrane (Bagnoli et al., 2005).

CagA induced loss of cell polarity is accompanied by two opposing phenotypes. Transient transgenic expression of CagA induces a transition from a polarized to an invasive phenotype where CagA expressing cells constrict the surface area of the apical membrane, form cell elongations and begin to migrate away from neighbouring cells underneath the remaining polarized epithelial cells (Bagnoli et al., 2005). CagA also induces an extrusion of epithelial cells towards the apical side causing a multi-layering phenotype (Saadat et al., 2007; Zeaiter et al., 2007). Both phenotypes are caused by CagA signalling motifs in the C-terminus of the protein.

Metastasis formation is a relatively late phenotype in malignant cancer and is often associated with a switch from a polarized, epithelial phenotype to a highly motile fibroblastic phenotype (epithelial-mesenchymal transition, EMT) (Huber et al., 2005).

CagA induces cell migration and cell invasion. However it is unclear to what extent CagA is able to induce EMT, the switch from a polarized, epithelial phenotype to a highly motile fibroblastic phenotype, a central process of cancer progression.

1.5 Aims of this work

A large proportion of ongoing research focuses on the C-terminal part of CagA with its EPIYA and CM/CRPIA motif with less emphasis being placed on the role of the N-terminal part of CagA. This work aims to clarify the role of the CagA N-terminus on host cell responses, by focusing on the CagA protein as a single factor. A tissue culture model was used to investigate the localization of CagA and mutant CagA proteins in polarized epithelial cells.

Diversity in CagA function could be regulated by differences in intracellular localisation to cellular substructures. CagA induced host signalling has been linked to plasma membrane localization of CagA. Yet it is unclear which part of CagA is responsible for the membrane localisation. Here, a novel membrane-binding domain of CagA will be presented and it’s role on host cell responses will be studied in a variety of functional assays.

Furthermore a second part of CagA was identified, which binds to a membrane structure in polarized epithelial cells independently of the membrane-binding domain.

The data presented in this work will show that the membrane-binding domain of CagA inhibits the migratory phenotype induced by the CagA C-terminus. The membrane-binding domain of CagA also increases cell-cell adhesion and inhibits TCF/b-catenin transcriptional activity mediated by C-terminus of CagA.

2 Materials and Methods

2.1 Laboratory Equipment

Instrument	Description
Branson Sonifier 250	Branson, CT (USA)
Centrifuge 5810R with 96-Well Plate adaptors	Eppendorf, Hamburg (Germany)
Gel doc XR+ documentation system	Bio Rad, Munich (Germany)
Gene Amp PCR System 9700	Applied Biosystems, Darmstadt (Germany)
Hera cell 240 CO_2 - incubator (Hereaus)	Thermo electronic corporation, Langenselbold (Germany)
Hera Safe KS18 Safety Cabinet (Hereaus)	Thermo electronic corporation, Langenselbold (Germany)
Leica SP5, confocal microscope	Leica, Wetzlar (Germany)
Lumat LB 9507 Luminometer	EGG Berthold, Bad Wilbad (Germany)
NanoDrop ND 1000	peqlab biotechnology GmbH, Nürnberg (Germany)
Odyssey infrared imaging system	Li-Cor, Bad Homburg (Germany)
Optima™ XL-100K Preparative Ultracentrifuge with Type 100 Ti rotor	Beckman Coulter, CA (USA)
Spectrophotometer (Smart Spec Plus)	Bio Rad, Munich (Germany)
Voltohmmeter (Millicell-ERS)	Millipore, Eschborn (Germany)
Plastic	**Description**
12mm Transwell® with 0.4µm Pore Polycarbonate Membrane Insert, Sterile	Corning, NY (USA)
12mm Transwell® with 0.4µm Pore Polyester Membrane Insert, Sterile	Corning, NY (USA)
8 Chamber Culture Slides (Falcon)	BD Labware, NY (USA)
Cell Scraper (24 cm, 38 cm)	Techno Plastic Products AG, Trasadingen (Switzerland)
Cloning Discs 5mm	Sigma-Aldrich, Steinheim (Germany)
Immobilon-FL 0.45-m PDVF membrane	Millipore, MA (USA)
Multiwell tissue culture plates (6-, 24-Well) (Falcon)	BD Labware, NY (USA)
Tissue culture dish (10cm, 15cm) (Falcon)	BD Labware, NY (USA)
Software	**Description**
GraphPad Prism	Graph Pad Software, CA (USA)
IMAGEJ software	National Institutes of Health, MD (USA)
Odyssey software 1.2.	Li-Cor, Bad Homburg (Germany)
Photoshop CS	Adobe Systems, CA (USA)
R project for statistical computing, R Version 2.8.1	GNU Project
Vector NTI	Invitrogen, Karlsruhe (Germany)
Volocity 4.1	Improvision, Coventry (England)

2.2 Reagents

2.2.1 Cell Culture Reagents

Reagent	Description
50 mg/ml Hygromycin B in PBS	Invitrogen, Karlsruhe, (Germany)
BD Matrigel™ Basement Membrane Matrigel, growth factor reduced, mouse natural	BD Bioscience, Heidelberg (Germany)
Doxycycline hyclate	Sigma-Aldrich, Taufkirchen (Germany)
Dulbecco's Modified Eagle Medium (D-MEM) (1X), liquid (high glucose)	Gibco, Karlsruhe (Germany)
Dulbecco's Modified Eagle Medium (D-MEM) (1X), powder (low glucose)	Gibco, Karlsruhe (Germany)
Dulbecco's Phosphate Buffered Saline (D-PBS) (1X), liquid	Gibco, Karlsruhe (Germany)
EDTA	Fluka, Seelze (Germany)
FBS Superior	Biochrom, Berlin (Germany)
Geneticin G-418 sulphate	Gibco, Karlsruhe (Germany)
Lipofectamine LTX Reagent	Invitrogen, Karlsruhe, (Germany)
Sodium bicarbonate, powder, ≥99.5% for cell culture	Sigma-Aldrich, Taufkirchen (Germany)
Opti-MEM® I Reduced-Serum Medium (1X), liquid	Gibco, Karlsruhe (Germany)
Trypsin, 2.5% (10X), liquid	Gibco, Karlsruhe (Germany)

2.2.2 Molecular biology and Biochemistry Reagents

Reagent	Description
10x PBS pH 7.4	Invitrogen, Karlsruhe, (Germany)
Ammonium persulphate (APS)	Roth, Karlsruhe, (Germany)
Antipain dihydrochloride, Leupeptin, Pepstatin	Roch, Penzberg (Germany)
Aprotinin	Sigma-Aldrich, Taufkirchen (Germany)
DL-Dithiothreitol (DTT)	Sigma-Aldrich, Taufkirchen (Germany)
LI-COR Blocking Buffer	LI-COR, Bad Homburg (Germany)
N, N, N', N'-tetramethylethylenediamine (TEMED)	Roth, Karlsruhe, (Germany)
N,N'-Methylenebisacrylamide (Bisacrylamid)	Roth, Karlsruhe, (Germany)
Phosphatase Inhibitor Cocktail 2	Sigma-Aldrich, Taufkirchen (Germany)
Prestained SDS-PAGE Standards, Broad Range	Bio Rad, Munich, (Germany)
Protein A/G Plus Agarose	Santa Cruz Biotechnology, CA (USA)
Sodium Dodecyl Sulfate (SDS)	Roth, Karlsruhe, (Germany)
Tween 20	Roth, Karlsruhe, (Germany)
VECTASHIELD® HardSet™ Mounting Medium with DAPI	Vector Lab., Inc., Burlingame, CA (USA)
VECTASHIELD® Mounting Medium with DAPI	Vector Lab., Inc., Burlingame, CA (USA)

2.2.3 Cloning

Reagent	Description
100Bp DNA-Ladder	Roth, Karlsruhe, (Germany)
6x Gel loading dye	Roth, Karlsruhe, (Germany)
2.5 mM dNTP Mix	Invitrogen, Karlsruhe, (Germany)
Agarose	Roth, Karlsruhe, (Germany)
Ampicillin sodium salt	Roth, Karlsruhe, (Germany)
Ethidiumbromide	Roth, Karlsruhe, (Germany)
Kanamycinsulphate	Roth, Karlsruhe, (Germany)
LB-Agar (Luria/Miller)	Roth, Karlsruhe, (Germany)
LB-Medium (Luria/Miller)	Roth, Karlsruhe, (Germany)
CIP- alkaline phosphatase	New England Biolabs (NEB), Frankfurt am Main (Germany)
One Shot® MAX Efficiency™ DH10B™ T1 Phage Resistant Cells	Invitrogen, Karlsruhe, (Germany)
Platinum® Taq DNA Polymerase	Invitrogen, Karlsruhe, (Germany)
Platinum® Taq DNA Polymerase High Fidelity	Invitrogen, Karlsruhe, (Germany)
Subcloning Efficiency™ DH5™ Competent Cells	Invitrogen, Karlsruhe, (Germany)
T4 DNA Ligase High Concentration	Invitrogen, Karlsruhe, (Germany)
UltraPure™ Agarose	Invitrogen, Karlsruhe, (Germany)
Zero Blunt® TOPO® PCR Cloning Kit	Invitrogen, Karlsruhe, (Germany)
Restriction Enzyme	**Description**
AgeI	NEB, Frankfurt am Main (Germany)
AhdI	NEB, Frankfurt am Main (Germany)
AscI	NEB, Frankfurt am Main (Germany)
BamHI	NEB, Frankfurt am Main (Germany)
EcoRI	NEB, Frankfurt am Main (Germany)
HindIII	NEB, Frankfurt am Main (Germany)
NheI	NEB, Frankfurt am Main (Germany)
NotI	NEB, Frankfurt am Main (Germany)
SalI	NEB, Frankfurt am Main (Germany)
XhoI	NEB, Frankfurt am Main (Germany)
XbaI	NEB, Frankfurt am Main (Germany)

2.2.4 Kits

Kit	Description
Dual-Luciferase Reporter Assay System	Promega, Mannheim, (Germany)
HiPure Plasmid Filter MidiPrep Kit	Invitrogen, Karlsruhe, (Germany)
Luciferase Reporter Assay System	Promega, Mannheim, (Germany)
QIAprep Spin Miniprep Kit (250)	Qiagen, Hilden (Germany)
QIAquick Gel Extraction Kit (50)	Qiagen, Hilden (Germany)
Tet On Advanced Inducible Gene Expression System	Clontech (Germany)

2.2.5 Medium and Buffers

Buffer	Composition
1x DMEM, 1g/L Glucose, 1g/L $NaHCO_3$	10g DMEM powder 1g $NaHCO_3$ pH 7,0 (HCL) Filtered sterile
1x TAE	40 mM Tris 20 mM acetic acid 1 mM EDTA pH 8.0
2x Quick Ligase buffer	132 mM Tris HCL 20 mM $MgCl_2$ 2 mM DTT 2 mM ATP 15 % PEG 6000
4x SDS Sample Buffer	0.8% SDS 160 mM Tris pH 6.8 30% Glycerol
Collagen quenching buffer	75 mM NH_4Cl 20 mM Glycin in PBS
Collagen solution	Dilution of 1:10 rat-tail collagen (extracted from rat-tails kindly provided by R. Vogelmann. For protocol see nelsonlab.stanford.edu/lab/labbible) In 1:1000 acetic acid
Fixative - 2% paraformaldehyde in 100 mM sodium phosphate buffer pH 7.4	Solution A - 100mM sodium phosphate, pH 7,4: 1M dibasic Na-phosphate pH 9 - 2430µl 1M monobasic Na-phosphate pH 4.1 - 570µl dH_2O - 27ml Solution is mixed in a proportion of 19:81 to get a pH of 7.4 Solution B - 8% paraformaldehyde pH 7.4 Solution A and B are combined 3:1
Homogenisation buffer	20 mM Hepes-KOH, pH=7.2 90 mM K-Acetate 2 mM Mg-Acetate 25 mM Sucrose Proteinase inhibitors Phosphatase inhibitor cocktail 2

Horse blood agar plates	Columbia Agar 740 µM Vancomycin 130 µM Cefsulodin 24 µM Polymixin B 29 µM Trimethoprim 142 µM Amphotericin B 2.2 mM β-cyclodexadrine
PBS-EDTA	1x DPBS, sterile 0.1 mM EDTA pH 7.4
PBS-Trypsin-EDTA	1x DPBS, sterile 0.07% Trypsin 0.1 mM EDTA pH 7.4
Permeabilization and Blocking Buffer for IF	PBS 3% BSA (bovine serum albumin) 1% Saponin 0.1% Triton X-100 0.05% Sodium Azide
Ringer's buffer	10 mM Hepes pH 7.4 154 mM NaCl 7.2 mM KCl 1.8 mM $CaCl_2$
SDS-Running buffer	192 mM Glycine 25 mM Tris 0.1% SDS
Transfer buffer	25 mM Tris 192 mM Glycine 20% V/V Methanol
Washing Buffer for IF	PBS 3% BSA (bovine serum albumin) 1% Saponin 0.05% Na Azide

2.3 Cell lines and bacterial strains

Cell line	**Origin**	**Description**
Madin Darby canine kidney II (MDCK II)	Canine kidney epithelium	W.J. Nelson (Stanford University, Stanford, CA)
AGS	Human gastric adenocarcinoma	American Type Culture Collection
NCI-N87	Human gastric adenocarcinoma	American Type Culture Collection

Helicobacter pylori strain	**Origin**	**Description**
G27-MA	Natural variant of G27 (clinical isolate from a patient with peptic ulcer disease) selected for increased adhesion and ability to deliver CagA to MDCK cells (Amieva 2002)	W.J. Nelson (Stanford University, Stanford, CA)

G27-$CagA_{EPISA}$	$CagA_{EPISA}$ expresses mutant CagA that cannot be tyrosine phosphorylated (Stein 2002)	W.J. Nelson (Stanford University, Stanford, CA)
G27-ΔCagA	CagA cannot be translocated into cells (Stein 2002)	W.J. Nelson (Stanford University, Stanford, CA)

2.4 Antibodies

Antibody	Clone	Concentration	Description
Mouse anti-Actin	AC-40	IB 1:1000	Sigma, Missouri (USA)
Mouse anti-b-Catenin	14	IF 1:200	BD Transduction Laboratories, Heidelberg (Germany)
Rabbit anti-active Caspase3		IF 1:500	Abcam, Cambridge (UK)
Mouse anti-Claudin-1		IF 1:200	Zymed Laboratories, Invitrogen, CA (USA)
Rabbit anti-CagANT		IF 1:1000 IB 1:3000	Made against the N-terminal domain of CagA. Recombinant CagA1-877 GST fusion protein expressed in E.coli. (Tan et al., 2009)
Mouse anti-E-cadherin	36	IF 1:200	BD Transduction Laboratories, Heidelberg (Germany)
Rabbit anti-GFP Alexa Fluor 488		IF 1:1000	Molecular Probes, Invitrogen, OR (USA)
Mouse anti-GP135		IF 1:20	Ojakian and Schwimmer, 1988
Rabbit anti-Occludin		IF 1:200	Zymed Laboratories, Invitrogen, CA (USA)
Mouse anti-Phosphotyrosin	PY20	IB 1:1000	BD Transduction Laboratories, Heidelberg (Germany)
Mouse anti-ZO1	1A12	IF 1:200 IB 1:1000	Zymed Laboratories, Invitrogen, CA (USA)
Rabbit anti-ZO1		IF 1:200	Zymed Laboratories, Invitrogen, CA (USA)
Alexa Fluor 488 phalloidin		IF 1:500	Molecular Probes, Invitrogen, OR (USA)
Alexa Fluor 594 phalloidin		IF 1:200	Molecular Probes, Invitrogen, OR (USA)
Alexa Fluor 647 phalloidin		IF 1:50	Molecular Probes, Invitrogen, OR (USA)
Alexa Fluor 488 Goat anti-Mouse		IF 1:200	Molecular Probes, Invitrogen, OR (USA)
Alexa Fluor 546 Goat anti-Mouse		IF 1:200	Molecular Probes, Invitrogen, OR (USA)
Alexa Fluor 594 Goat anti-Mouse		IF 1:200	Molecular Probes, Invitrogen, OR (USA)
Goat anti-Mouse IgG		IF 1:200	Pierce Biotechnology, IL (USA)

Dye Light 649		
Alexa Fluor 488 Goat anti-Rabbit	IF 1:200	Molecular Probes, Invitrogen, OR (USA)
Alexa Fluor 546 Goat anti-Rabbit	IF 1:200	Molecular Probes, Invitrogen, OR (USA)
Alexa Fluor 594 Goat anti-Rabbit	IF 1:200	Molecular Probes, Invitrogen, OR (USA)
Alexa Fluor 647 Goat anti-Rabbit	IF 1:200	Molecular Probes, Invitrogen, OR (USA)
Alexa Fluor 680 Goat anti-Mouse	IB 1:30,000	Molecular Probes, Invitrogen, OR (USA)
Alexa Fluor 680 Goat anti-Rabbit	IB 1:30,000	Molecular Probes, Invitrogen, OR (USA)
Anti-Rabbit IgG IRDye 800	IB 1:30,000	Rockland, PA (USA)
Anti-Mouse IgG IRDye 800	IB 1:30,000	Rockland, PA (USA)

2.5 Cell Culture Methods

2.5.1 Maintenance of cell lines

MDCK II, AGS and NCI-N87 cells were cultured in DMEM low Glucose containing 1g/l $NaHCO_3$, DMEM high Glucose or RPMI supplemented with 10% fetal bovine serum in an incubator at 37°C, 5% CO_2 and 100% humidity. At a confluence of 90% cells were split 1:10 by washing one time with PBS-EDTA and adding PBS-Trypsin-EDTA until cells detached from cell culture dish. Trypsination was blocked by adding culture medium with 10% FBS and cells were collected in a 15 ml centrifugation tube. Cells were spun down at 1000rpm for 4 minutes, re-suspended in fresh culture medium and seeded on a new culture dish.
For the maintenance of stable cell lines, 400 µg/ml Genetecin-G418 and 150 µg/ml Hygromycin B were added to culture medium.
For induction of protein expression 3µg/ml doxycycline (dox) were added to culture medium.

2.5.2 3D-Cell Culture

Preparation of bottom layer:
Matrigel solidifies at room temperature hence every step was made on ice. 40µl drops of matrigel were applied on the centre of 4 wells of an 8-well chamber slide. To get a flat layer of matrigel, chamber slides were centrifuged on ice-cold 96-well plate adaptors for 10 min at 300 rfc at room temperature. Afterwards the matrigel was placed in a cell culture incubator for 10 minutes until it solidified.

Preparation of upper layer:
$5x10^4$ cells were re-suspended in 2 ml culture medium containing 2.5% matrigel. 400 µl/well of the cell suspension were applied on the matrigel bottom layer. Cysts then grow on the bottom layer. The culture medium was changed every 4 days, always containing 2.5% matrigel.

2.5.3 Transfection

Standard protocol:
All transfections were carried out by using Lipofectamine LTX from Invitrogen.
Twenty-four hours prior to transfection $1x10^5$ cells/well for 24 well plates ($5x10^5$cells/well for 6-well plates) were seeded. 0.5 µg (2.5 µg) DNA was diluted in

100 µl (500 µl) Opti-MEM, then 1.25 µl (6.25 µl) Lipofectamine was added and incubated for 30 minutes at room temperature. Culture medium was replaced with 0.5 ml (2.5 ml) fresh culture medium and the transfection reaction was added to the cells.

Transfection of polarized monolayers in transwell filters:

Forty-eight hours prior to transfection $5x10^5$ cells/Transwell filter (12-mm well, 0.4 µm pore size, polycarbonate membrane, collagen coated) were seeded. After 24 hours medium was changed. 2.5 µg DNA was diluted in 500 µl Opti-MEM, then 6.25 µl Lipofectamine were added and incubated for 30 minutes at room temperature. The culture medium in the upper and lower compartment was replaced with 0.3 ml and 1.5 ml fresh culture medium supplemented with 3 µg/ml Doxycycline. The transfection reaction was then added to cells. After 24 hours cells were fixed and transferred to immunofluorescence staining.

Transfection of stable cell lines

Twenty-four hours prior to transfection $5x10^5$ cells/well were seeded on a 6-well plate. 2.5 µg DNA was diluted in 500 µl Opti-MEM, then 6.25 µl Lipofectamine was added and incubated for 30 minutes at room temperature. Culture medium was replaced with 2.5 ml fresh culture medium and the transfection reaction was added to cells. After 24 hours cells were split onto three 150-mm dishes with 20 ml culture medium containing selective antibiotics. After 14 days, large colonies were isolated by washing the culture dish with PBS-EDTA. Cloning discs were soaked in PBS-EDTA-Trypsin and placed on colonies for 10 minutes. Cloning discs were then transferred to 24-well plates and single cell clones were expanded.

2.5.4 Stable MDCK cell lines expressing CagA and CagA mutants

MDCK Teton Advanced cell line:

The pTet-On-Advanced vector encodes the transactivator that binds TRE-Tight in the presence of Doxycycline. MDCK cells, stably expressing rtTA-Advanced, were selected according to the protocol for transfection of stable cell lines.

MDCK cells were transfected with pTet-On-Advanced Vector, which contains a Genetecin-G418 resistance marker. Selected clones were co-transfected with the pTRE-Tight-Luc Vector and screened for clones with high luciferase activity using the Luciferase Assay System from Promega according to the manufacturer's protocol (selected clone TetonA#19).

Stable CagA cell lines:

pTRE-tight-GFP-CagA constructs were transfected into the TetonA#19 cell line and selected via co-transfection of a linear hygromycin marker at a ratio 1:10 according to the protocol for transfection of stable cell lines.

Selected clones were screened for GFP expression. $1x10^5$ cells were seeded on 24-well cover slides and protein expression was induced for 24 hours. Cells were analyzed for protein expression via immunofluorescence. Clones with at least 80% expressing cells were selected and expanded. Expression of the correct size of CagA protein of was verified by immunoblotting.

2.5.5 Infection of MDCK cysts with Helicobacter pylori

H. pylori from a frozen stock was streaked onto a pre-warmed horse blood agar plate. Plates were incubated for 1 to 2 days before the bacteria were used for inoculation of confluent MDCK cells (infection medium: DMEM containing 10% FBS, 10% Brucella Broth and 10µg/ml Vancomycin). *H. pylori* solution from a co-culture was used for infection of MDCK cysts. Since *H. pylori* doesn't grow in colonies, the optical density at wavelength 593 nm (OD_{593}) was calculated and cysts were infected with *H. pylori* solution at an OD_{593} = 0.1.

2.6 Immunofluorescence staining

Collagen coating of cover slips and Transwell filters:

Cover slips were singly placed in 24-well cell culture plates. The collagen solution (1:10 rat tail collagen in 1:1000 acetic acid) was applied onto cover slips or transwell filters in the upper and in the lower compartment and incubated for 5 minutes. The collagen solution was removed and the culture plates were placed under UV-light for 60 minutes to dry and sterilise the cover slips and transwell filters.

Immunofluorescence staining of cover slips and transwell filters:

Cells were grown on collagen coated cover slips or transwell filters. The optimal induction time for CagA expression was 24 hours. Cells were washed once with PBS and fixed with Fixative for 10 minutes. Fixative was removed and cells were washed 3 times with PBS. Transwell filters were cut out of the permeable support with a scalpel. Cover slips and transwell filters were transferred to a humidified chamber (dark box with parafilm and wet paper towels) and permeabilized in Permeabilization buffer for 10 min at room temperature. Antibodies were diluted in washing buffer and

incubated for 1 hour at room temperature. After incubation, antibody solution was removed and cells were washed 3 times for 5 minutes with washing buffer. Before mounting, cells were washed once with PBS. Cells were mounted with Vectashield and sealed with nail polish.
After staining, samples were imaged with a confocal microscope, arranged by using Volocity software and assembled with Photoshop.

Immunofluorescence staining of 3D-Cysts:

The cysts, which grew on matrigel in 8- well chamber slides, were washed 3 times with PBS for 5 min before fixation with fixative for 3 hours. To reduce background during imaging, collagen quenching buffer was added for 10 minutes. Cysts were then permeabilized for 3 hours. Antibodies were incubated over night at 4°C. After incubation, antibody solution was removed and cells were washed 3 times for 30 minutes with washing buffer. Before mounting, cells were washed 3 times with PBS for 30 minutes. Cells were mounted with Vectashield Hard Set and sealed with nail polish.

2.7 Biochemistry Methods

2.7.1 Cloning of Expressions Vectors

2.7.1.1 Protocols for cloning

PCR Reaction:

10X High Fidelity Buffer	5µl
dNTP mix 2,5mM each	4µl
50 mM $MgSO_4$	2µl
Forward Primer	0.5µl
Backward Primer	0.5µl
Template DNA	1µl
Taq DNA Polymerase HF	0.2µl
dH_2O	36.8µl

Cycling Parameters:

Denaturation 94°C 2 min

Denaturation	94°C	30sec	30 Cycles
Annealing	64°C	30 sec	
Extension	72°C	30 sec	

Final Extension 72°C 7 min

Gel electrophoresis for control of PCR products and restriction digests:

1% Agarose gels (ultrapure agarose for cloning) in TAE buffer with 2 µl Ethidium-bromide were prepared. Probes were prepared with 6x gel loading dye. For comparison of band size a 100Kb DNA-marker was used. Electrophoresis was performed at 120mV (80mV for ultrapure agarose). Agarose gels were imaged with the gel doc XR+ documentation system from BioRad.

TOPO cloning reaction:

Fresh PCR Product	1 µl
Saltsolution	1 µl
Sterile Water	3 µl
pCRII-Blunt-TOPO	1 µl → Mix and incubate 5 minutes at room temperature

Digest reaction for TOPO clones:

DNA	0.5 µl	
EcoR1	0.1 µl	
BSA	2 µl	
10X EcoR1 Buffer	7.4 µl	
H_2O	10 µl	→1 hour at 37°C water bath

Digest reaction for cloning:

DNA	0.5µg
Restriction enzyme 1	0.5µl
Restriction enzyme 2	0.5µl
BSA	2µl
10X EcoR1 Reaction Buffer	2µl
H_2O	added to 20 µl

Digest reaction for control of plasmids:

DNA	0.5µl	
Restriction Enzyme	0.2µl	
BSA	1µl	
10X Reaction Buffer	1µl	
H_2O	7.3µl	1 hour at 37°C water bath

The digest reaction was separated by gel electrophoresis and correct DNA fragments were cut from gel and purified using the Qiagen Gel Extraction Kit according to the manufacturer's instructions using 30 µl TE-Water for elution.

Quick Ligation Reaction:

Quick Ligation Buffer	10µl	
Vector DNA	2.5µl	
Insert DNA	7.5µl	
Ligase HC	1µl	→ 10 minutes at room temperature

Transforming competent cells DH10B/ TOP10/ DH5α:

2 µl of the ligation reaction (1µl DNA) was added to competent cells and mixed carefully. Cells were incubated on ice for 30 minutes. The cells were heat shocked in a 42°C water bath for 30 seconds and then put on ice for 2 minutes. 250 µl of S.O.C. medium (750µl LB-medium) was added and cells were incubated at 37°C with shacking for 1 hour. Next, cell solution was put on selection agar plates with appropriate antibiotics over night at 37°C.

Colonies were picked and grown in 3 ml LB Medium supplemented with appropriate antibiotics overnight.

DNA was isolated using the Qiagen Miniprep Kit according to manufacturer's instructions.

2.7.1.2 Cloning of CagA mutants with various amino acid lengths

CagA constructs were generated by cloning PCR products from a previously published pEGFP-CagA wt plasmid (*H. pylori* strain G27) (Bagnoli et al., 2005) into a modified pTRE-tight Vector from Clontech.

Primers were designed using Vector NTI (Invitrogen) and purchased from Eurofins (Germany).

CagA construct	Restriction site	Primer forward	Primer backward
pTREtightGFPSBP	BamHI_SalI/NotI	gga tcc cgc cac cat ggt gag caa gg	gcg gcc gca gac ata cgt gtc gac ctt gta cag ctc gtc cat gcc
CagA 1-200	SalI_NotI	gtc gac gtg act aac gaa acc att aac caa	gcg gcc gcc att ttt ttc tgc ttc ttg cct tt
CagA1-150	SalI_NotI	gtc gac gtg act aac gaa acc att aac caa	gcg gcc gcg gat agg ggg ttg tat gat att t
CagA25-225	SalI_NotI	gtc gac gtg gct ttt ctt aaa gtt gat aac	gcg gcc gct gac atc aga aga ttg ttt ttt gtc
CagA400-800	SalI_NotI	gtc gac aat ttc ttg cac aaa ata atg ctg	gcg gcc gct gaa atc acc cgt tgc ttt agc
CagA 200-800	SalI_NotI	gtc gac ggg cct act ggt ggg gat tg	gcg gcc gct gaa atc acc cgt tgc ttt agc
CagA1-800	SalI_NotI	gtc gac gtg act aac gaa acc att aac caa	gcg gcc gct gaa atc acc cgt tgc ttt agc
CagA800-1216	NotI_XbaI	gcg gcc gca gta ggg tag agc aag cgt ta	tct aga aag att ttt gga aac cac ctt ttg
CagΔPar1 PCR1	Nhe_AscI	agc tag ccc tga aga acc cat	tgg cgc gcc tgc cca ctg ctt gcc cta caa
CagΔPar1 PCR2	Nhe/AscI_NotI	gct agc acg tat gtc tgg cgc gcc ctt tca agg gag caa caa ttg a	tgc ggc cgc aag att ttt gg
CagA800-1216EPISA	NotI_XbaI	gcg gcc gca gta ggg tag agc aag cgt ta	tct aga aag att ttt gga aac cac ctt ttg

The pTRE-tight vector from Clontech was modified as follows:

pTRE-tight-SBP was cloned by introducing a SBP/CBP (SBP) tag from Stratagene vector pCTAP at the C-terminus via NotI/XbaI.

GFP-CagA wt from the previously published pEGFP-CagA wt plasmid was inserted in frame via BamHI/NotI into the modified pTRE-tight-SBP vector.

pTRE-tight-GFP-SBP was cloned by introducing GFP from a EGFP Vector (Clontech) into pTRE-tight-SBP via BamHI/NotI.

The CagA constructs 1-200, 25-225, 1-150, 200-800 and 400-800 were cloned by inserting PCR products into pTRE-tight-GFP-SBP via SalI/NotI.

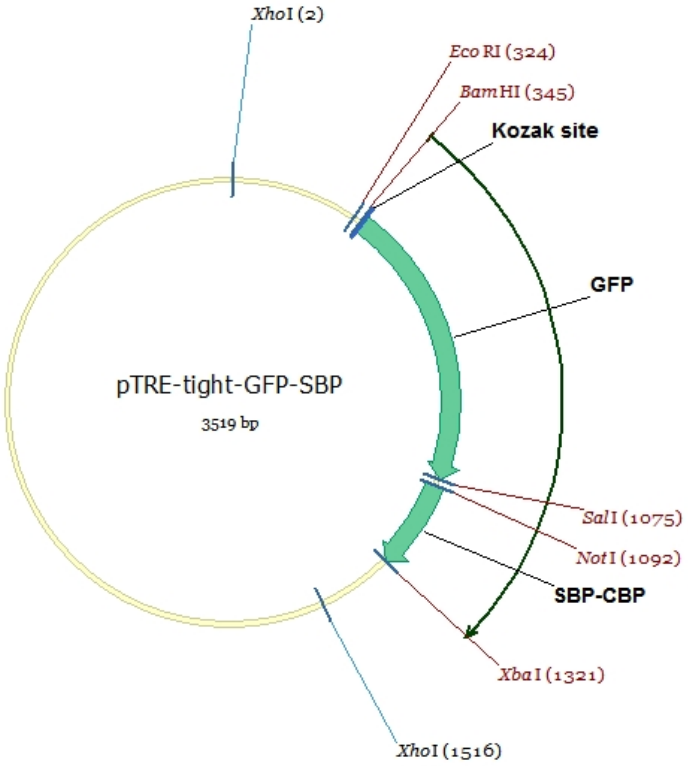

Figure 5: pTRE-tight-GFP-SBP. The SalI-NotI restrictions sites are used to clone CagA mutants in frame.

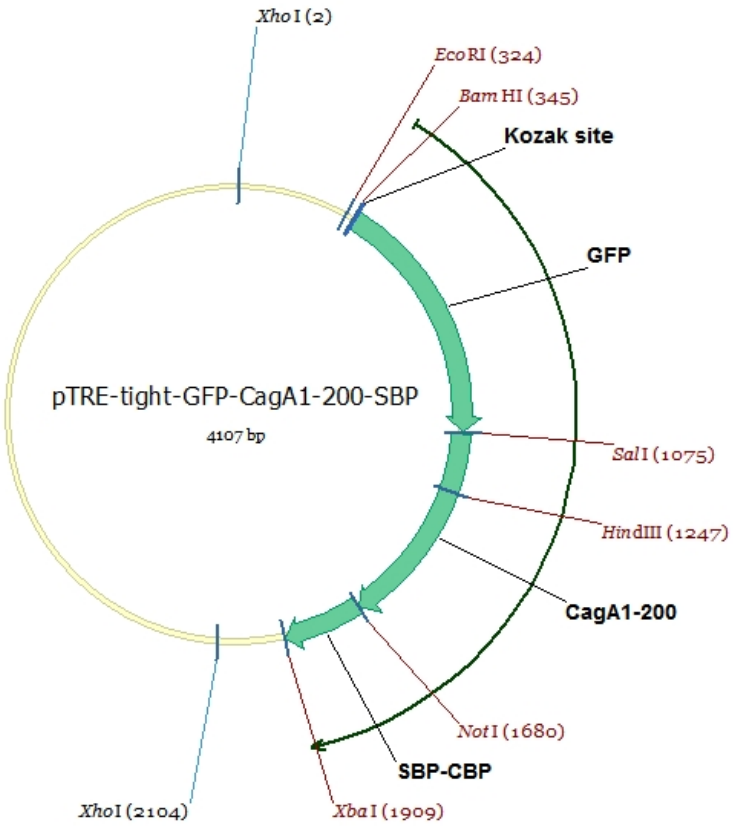

Figure 6: Example of a CagA mutant. CagA 1-200 was amplified by PCR from a pEGFP-CagA wt plasmid and cloned into pTREtight GFP via SalI/NotI.

For cloning of CagA 200-1216, CagA 400-1216 and CagAΔ200-800 the SBP- tag was replaced with CagA 800-1216 via NotI/XbaI. Utilising this method, CagA 1-200, 200-800 and 400-800 could be placed before the CagA 800-1216 via SalI/NotI. CagA 871-1216 mutant was cloned accordingly to CagA 800-1216 and was modified by replacing EGFP with monomeric RFP (Campbell et al., 2002).

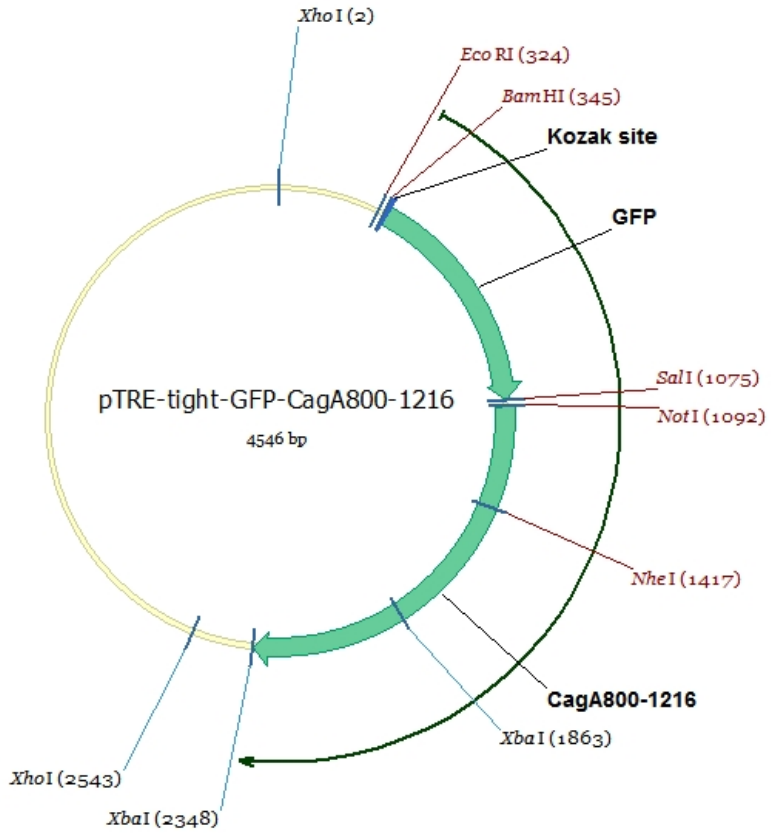

Figure 7: pTREtightGFPCagA800-1216. This Vector was used to clone CagA constructs containing the C-terminal part and various N-terminal parts of CagA.

2.7.1.3 CagAΔPar1

CagA FLΔPar1 was cloned by introducing an Asc1 restriction site before the first CM motif via PCR (NheI_AscI) into CagA wt via TOPO. The sequence 943-1027 containing the three CM and two EPYA (C) motifs was deleted via a second PCR (NheI/AscI_NotI). This was then cloned via NHE1/Not1 into the CagA wt plasmid.

1. PCR: fwd-NheI bwd-AscI Product: NheI---AscI
2. PCR: fwd NheI_AscI - (starting after last CM motif) bwd NotI (starting from end)

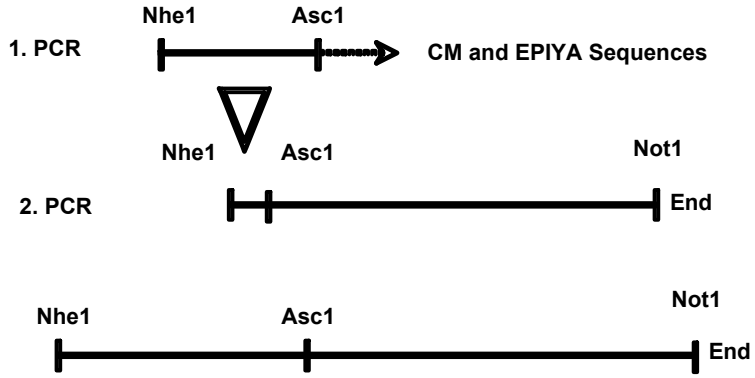

Figure 8: Cloning of ΔPar1. PCR products 1 and 2 were cloned into a TOPO plasmid and sequenced. The bridge of the second PCR product was replaced by the first PCR product via Nhe1/Asc1. Then the second PCR product was cloned into CagA wt via NheI/NotI deleting the CM motifs and EPISA (C) motifs.

CagA 800-1216 ΔPar1 was cloned by replacing the fragment between NheI/AhdI in the CagA 800-1216 mutant with the corresponding NheI/AhdI fragment from CagA ΔPar1.

CagA 200-1216 ΔPar1 was cloned by replacing the fragment between NheI/AgeI in the CagA 200-1216 mutant with the corresponding NheI/AgeI fragment from CagA 800-1216 ΔPar1.

2.7.1.4 CagA EPISA and CagA EPISA C

CagA EPISA C was chemically synthesized from bp 2830 to 3165 (AA 943 to 1055). Due to technical requirements synthesis of the EPISA C fragment required a change in codon usage (from canines familaris) optimized by "GENEius software" (Eurofins, Germany). The newly synthesised sequence was cloned into CagA FLΔPar1 and CagA CTΔPar1 via AscI/XbaI.

2830	TTTCCGCTGA	AACGCCATGA	CAAGGTAGGC	GATCTGTCGA	AAGTGGGGCA
2880	ATCAGTGTCC	CCTGAGCCAA	TTAGCGCCAC	AATCGACGAT	CTCGGTGGAC
2930	CTTTCCCACT	CAAGAGGCAC	GACAAGGTTG	GGGATCTGAG	CAAGGTCGGC
2980	TTAAGCGTCT	CTCCTGAGCC	CATATCTGCG	ACCATCGATG	ACTTGGGTGG
2030	ACCCTTTCCC	CTTAAGAGAC	ACGACAAAGT	GGGAGATCTG	TCCAAAGTCG
3080	GGCTAAGTCG	GGAACAGCAG	CTGAAGCAGA	AGATCGACAA	CCTCAGTCAG
3030	GCAGTGTCCG	AAGCCAAAGC	TGGCTTCTTC	GGCAA	

For CagA 800-1216 EPISA a PCR product of the C-terminus of *H. pylori* mutant strain CagA FLEPISA (Bagnoli et al., 2005) starting at AA 800 was used to replace CagA 800-1216 via NotI/XbaI. CagA 200-1216 EPISA was cloned by replacing the fragment between NheI/AgeI in CagA 200-1216 with the corresponding NheI/AgeI fragment from CagA 800-1216 EPISA mutant.

2.7.2 Immunoblotting

Protein Samples:

For verification of phosphorylation of CagA EPIYA motifs, MDCK cells expressing CagA and CagA mutants were washed 3 times with Ringer's buffer, scraped off with 2% CHAPS in homogenization buffer, incubated for 2 hours with rotation and centrifuged for 10 minutes at 4°C. Supernatant was collected and boiled in SDS-sample buffer containing dithiothreitol (DTT) (final concentration, 50 mM).

For verification of correct expression of CagA protein, MDCK cells expressing CagA and mutant CagA were washed 3 times with PBS and detached from culture plates with a cell scrubber in SDS-sample buffer containing DTT and boiled for 10 minutes. Protein samples were then separated in SDS polyacrylamide gels.

Gel electrophoresis:

SDS polyacrylamide gels were made after following protocol:

	Stacking Gel	7,5% Resolving Gel	10%Resolving Gel	14%Resolving Gel
dH_2O	3.8 ml	2.8 ml	2.2 ml	1.06 ml
1M Tris pH 8,7	-	2.98 ml	2.98 ml	2.98 ml
1M Tris pH 6,8	0.64 ml	-	-	-
10% SDS	50 µl	80µl	80µl	80µl
Bisacrylamid	0.5 ml	2 ml	2.7 ml	3.7 ml
100% TEMED	5 µl	4 µl	4 µl	4 µl
10% APS	25 µl	27 µl	27 µl	27 µl

The electrophoresis was performed with the BioRad electrophoresis system containing SDS-Buffer at 50 Volt for 30 minutes followed by 100 Volt for 120 minutes at room temperature.

Transfer:

Following electrophoresis, the separated proteins were transferred to Immobilon-FL 0.45-m PDVF membranes in a BioRad electrophoresis system containing transfer buffer at 100 Volt for 1 hour at 4°C.

Blocking and Detection:

Proteins were blocked with LI-COR blocking buffer in PBS (1:1) for 1 h at room temperature. Primary antibodies and fluorescence labelled secondary antibodies (1:30,000) were diluted in T-PBS (PBS containing 0.1% Tween 20) and incubated for 1 h at room temperature. Membranes were scanned with the Odyssey infrared imaging system at 680-nm and 800-nm wavelength. The amount of protein per fraction was determined by Odyssey software 1.2.

2.7.3 100.000g spin

MDCK cells stably expressing CagA mutants (1 x 10^8 cells in two 150-mm dishes) were washed 3 times with PBS before transfer into detergent free homogenization buffer. Cells were mechanically broken via Branson Sonifier 250 at 4ºC (Duty Cycle: 50%, Output control at Microtiplimit, level 1 for 15 secundes, pause 1 minute, level 2 for 10 seconds). After centrifugation at 100,000 x g for 45 minutes at 4ºC in a Beckman Coulter Type 100 Ti rotor, supernatant was removed and pellet was re-suspended in equal volume of homogenization buffer. Respective protein samples were boiled in SDS-sample buffer DTT for 10 min and separated in SDS polyacrylamide gels

2.8 Functional Assays

2.8.1 β-Catenin Activation

N87 cells were cultured in 24-well plates and grown to 60% confluence. Cells were co-transfected with 100 ng Topflash, 100 ng Fopflash, 100 ng pTeton-Advanced and 300 ng pTRE-Tight-CagA-wt and pTRE-Tight-CagA-200-1216 constructs, respectively using Lipofectamine LTX. CagA expression was activated using 3µg/ml dox. After 24 hours, cells were harvested in 100 µl reporter lysis buffer and luciferase activity was determined in a dual channel luminometer according to manufacture's protocol for Dual Luciferase Reporter Assay System (Promega). Results were normalized for transfection efficiency by cotransfection of the renilla luciferase plasmid.

2.8.2 Apical Constriction

CagA constructs were transiently transfected into polarized MDCK cells in transwell filters (12-mm well, 0.4 µm pore size, polyester membrane, collagen coated). To measure the perimeter of cellular junctions, the monolayers were stained with

antibodies to ZO-1 and transfected cells were identified through GFP fluorescence. The confocal optical sections from random fields were collapsed into single projections. IMAGEJ software was then used to select and measure the apical surface of individual cells. The data was transferred to an EXCEL worksheet and statistical analysis was performed using GraphPadPrism.

2.8.3 Hanging Drop Adhesion Assay

The assay was performed as described before (Ehrlich et al., 2002). In brief, MDCK stable cell lines were grown at low density and CagA mutant expression was induced as appropriate. Cells were trypsinized, centrifuged, and re-suspended as single-cell suspensions at 2.5 x 10^5 cells/ml. Twenty micro litre drops of cell suspension were pipetted onto inside lids, and dishes were filled with 2 ml of media to prevent evaporation. At 2 and 4 hours, the lid was inverted and drops were spread onto a glass slide. Drops were triturated ten times through a 20 µl pipette. At each time point three drops were photographed and the number and the size of clusters was determined.

2.8.4 Transepithelial Electrical Resistance

MDCK cells form polarised monolayers when seeded in high density on Transwell filters (12-mm well, 0.4 µm pore size, polyester membrane, collagen coated). The formation of the apical junctional complex can be followed by measuring the flux of ions in the culture medium.

Cells were seeded at a density of 5x10^5 cells/Transwell filter. For induction of CagA expression 3µg/ml doxycycline was added to the culture medium. For control, the cells were seeded without doxycycline.

The transepithelial electrical resistance (TER) of the epithelial monolayers was measured using a Millicell-ERS volt ohmmeter (Millipore, Eschborn). The electrodes were soaked in 12 ml of 80 % ethanol for 15 min in a 15 ml centrifuge tube, air dried for 30 sec and equilibrated with 7 ml of DMEM for another 15 min prior to use. Each Transwell insert was measured three times at different positions and the mean ± SD value was calculated. TER was followed for 24 hours.

2.9 Statistics

The mean values and SEMs were calculated from at least three different experiments. For the statistical analysis the Student's T-Test, the Cochran–Mantel–

Haenszel test or the Wilcoxon Signed Rank Test was used as it is marked in the figures and statistical significant was considered with a p-Value < 0.05. The software **R 2.8.1** for Mac OS X (Softliste.de, Berlin) and GraphPad Prism (Graph Pad Software) was used.

3 Results

3.1 MDCK cells as an *in vitro* model system for gastric epithelium

To study CagA as a single factor *in vitro*, a tissue culture model for gastric epithelial cells was required, but to date there is no suitable tissue culture model available for non-transformed human gastric epithelial cells. AGS cells, which are derived from a human gastric adenocarcinoma, are often used as a model system for gastric epithelium. However, AGS cells do not form proper junctions since they do not express E-Cadherin and have a constitutively active TCF/LEF signalling. Hence they are not applicable to study effects in polarised epithelium.

Madine Darby Canine Kidney (MDCK) cells are very well characterized and are the best-known tissue culture model for polarized epithelium. Although they are derived from the kidneys of a dog they share the same features as all epithelial cells. They form polarized monolayers with an intact AJC and develop a proper barrier function. After polarisation they down-regulate cell proliferation and migration. They also do not have mutations in the TCF/LEF pathway (Barth et al., 1997). Therefore MDCK cells were chosen as a model system for this work.

For stable and inducible expression of CagA and CagA mutant constructs in MDCK cells, the Tet-On® advanced Inducible Gene Expression System from Clontech was used. The Tet-Off/Tet-On advanced mammalian gene expression system is based on the E. coli tetracycline (tet) repressor system. The bacterial tet operon mediates transcriptional repression of a promoter in the presence of the tet repressor protein. Transcriptional repression is relieved by exposure to tetracycline, which binds to tet repressor protein and thereby prevents its interaction with the tet operon.

For the Tet-On Advanced System the regulatory proteins are based on a mutant reverse tet repressor that binds the tet operator sequence (tetO) in the presence of dox. The transactivator (rtTA-Advanced) activates transcription from a tetracycline response element (TRE) as a consequence of dox treatment. The TRE sequence consists of several repeats of the tetO and is located upstream of a minimal CMV promotor. The Teton Advanced expression system allows exclusion of clonal variances between the CagA expressing and non-expressing cells in experiments, since effects of CagA can be followed in the identical cell line in the uninduced and induced state. In this work CagA mutants with different amino acid lengths were

generated and stably transfected into MDCK cells to study the different domains of CagA (Figure 9). (For cloning strategy see 2.7.1)

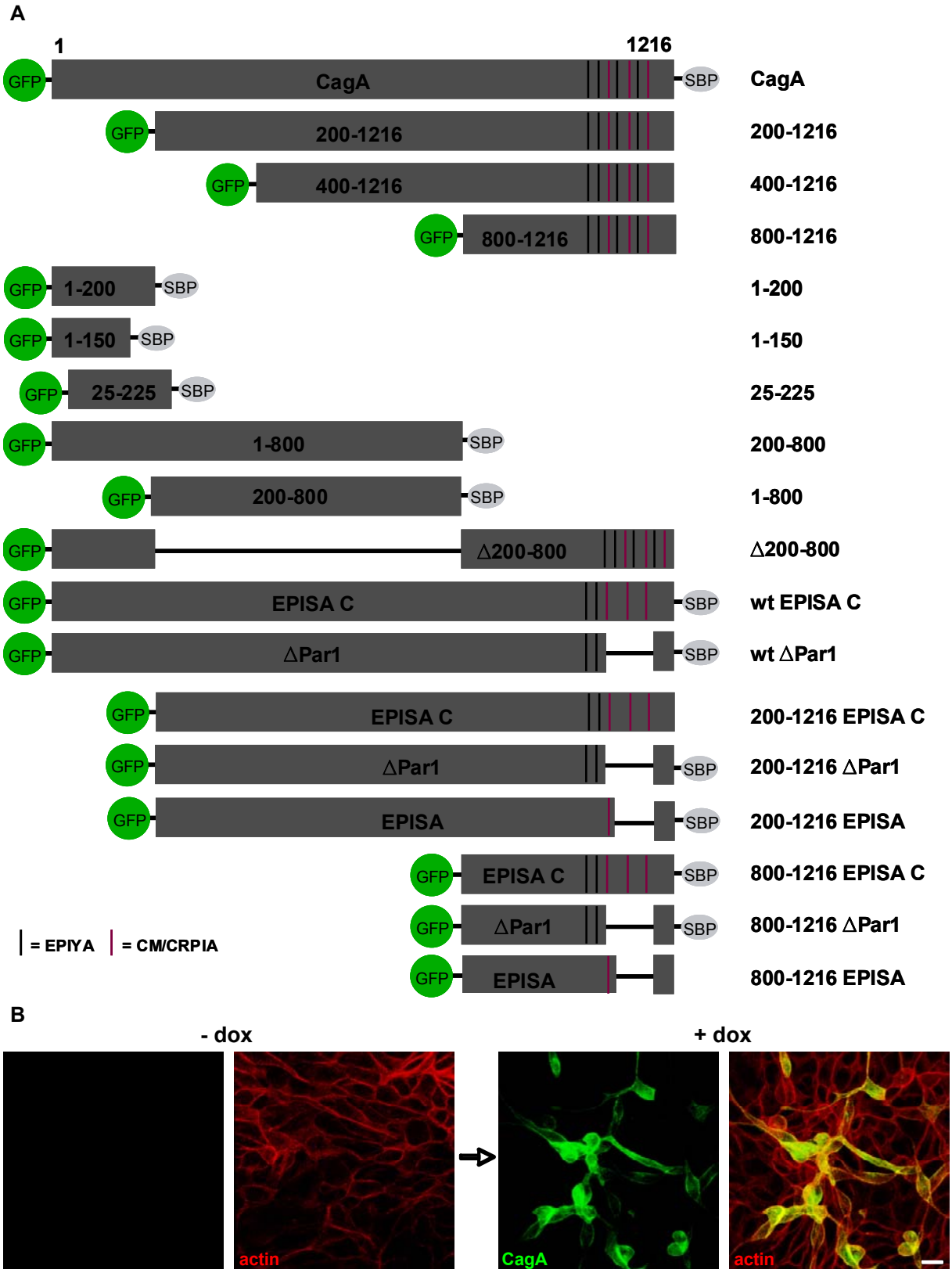

Figure 9: MDCK cells stably expressing CagA. A) Model of CagA constructs. B) Left panel without induction of protein expression, right panel CagA expression is induced by adding doxycycline to culture medium.

3.2 Identification of the Membrane Binding Domain of CagA

Publications state that CagA (CagA 1-871) interacts with the plasma membrane independently of the CagA C-terminus (Bagnoli et al., 2005). To identify the least amount of amino acids required for membrane targeting of CagA, CagA mutant constructs were created with decreasing amino acid lengths. CagA 1-200 was identified as the shortest amino acid sequence that localises to the membrane (Figure 10A) and therefore defined as CagA Membrane Binding Domain (MBD).
A CagA mutant shorter then 200 AA (CagA 1-150) or a mutant lacking the first 25 AA (CagA 25-225) is distributed throughout the cytoplasm (Figure 10C,D).

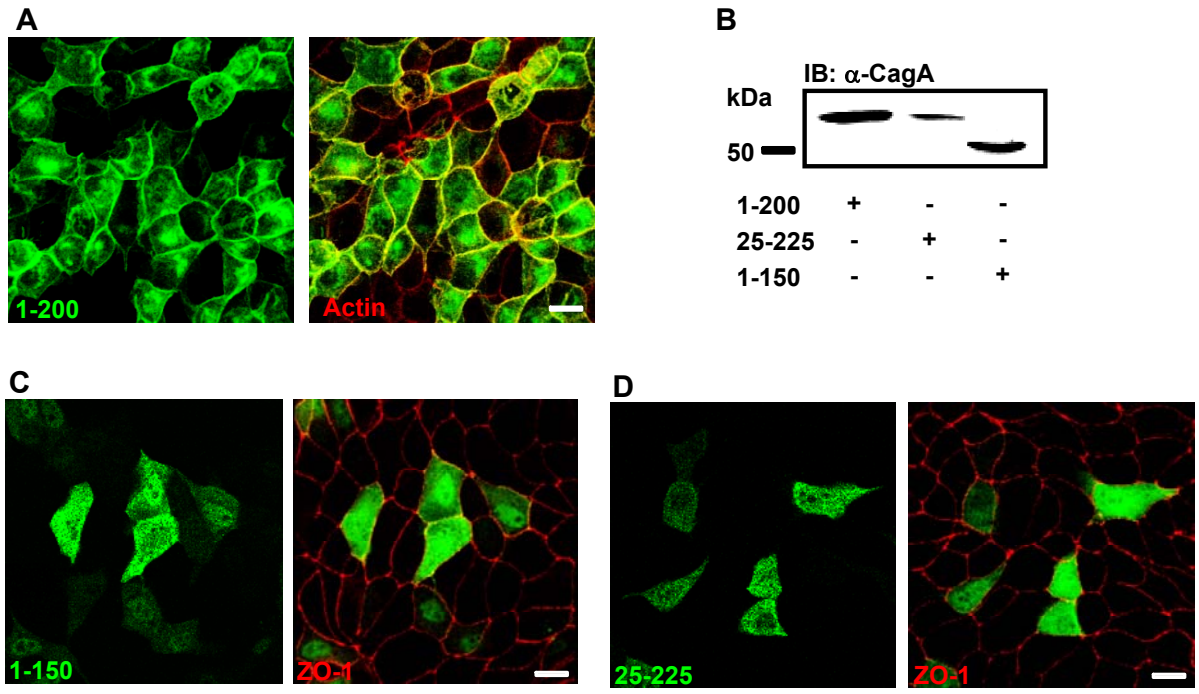

Figure 10: Membrane localistaions of CagA 1-200. A) Confocal microscopy images of GFP CagA 1-200 (green) expressing cells. 3-D reconstructions of confocal z-stacks. Non-polarized cells. Left: GFP- CagA 1-200 (green). Right: actin staining (red). Bar 10µm. B) IB of CagA 1-200, CagA 25-225 and CagA 1-150. C and D) Confocal microscopy images of GFP CagA (green) expressing cells and ZO-1 staining (red). Left panels: x-y plane. Right panels: 3-D reconstructions of confocal z-stacks. Non-polarized cells: CagA 1-150 and CagA 25-225 are localised to the cytoplasm. Bar 10µm.

3.2.1 Localisation of CagA MBD to specific membrane substructures.

In non-polarized cells, CagA 1-200 is enriched at cell-cell contact sites co-localising with the cadherin/catenin protein complex at the lateral membrane (Figure 11A,B) and in lamellipodia at forming cell-cell contact sites (Figure 11C). Lamellipodia initiate cadherin-mediated contacts between cells via E-cadherin clustering and subsequent expansion of contacts to form strong cell-cell adhesion (Ehrlich et al., 2002; Yamada and Nelson, 2007). CagA 1-200 is excluded from membrane sites not engaged in

cell-cell contacts (see ➤ in Figure 11A). When expressed in polarized epithelial cells, CagA 1-200 localizes along the apical and lateral membrane (Figure 11D).

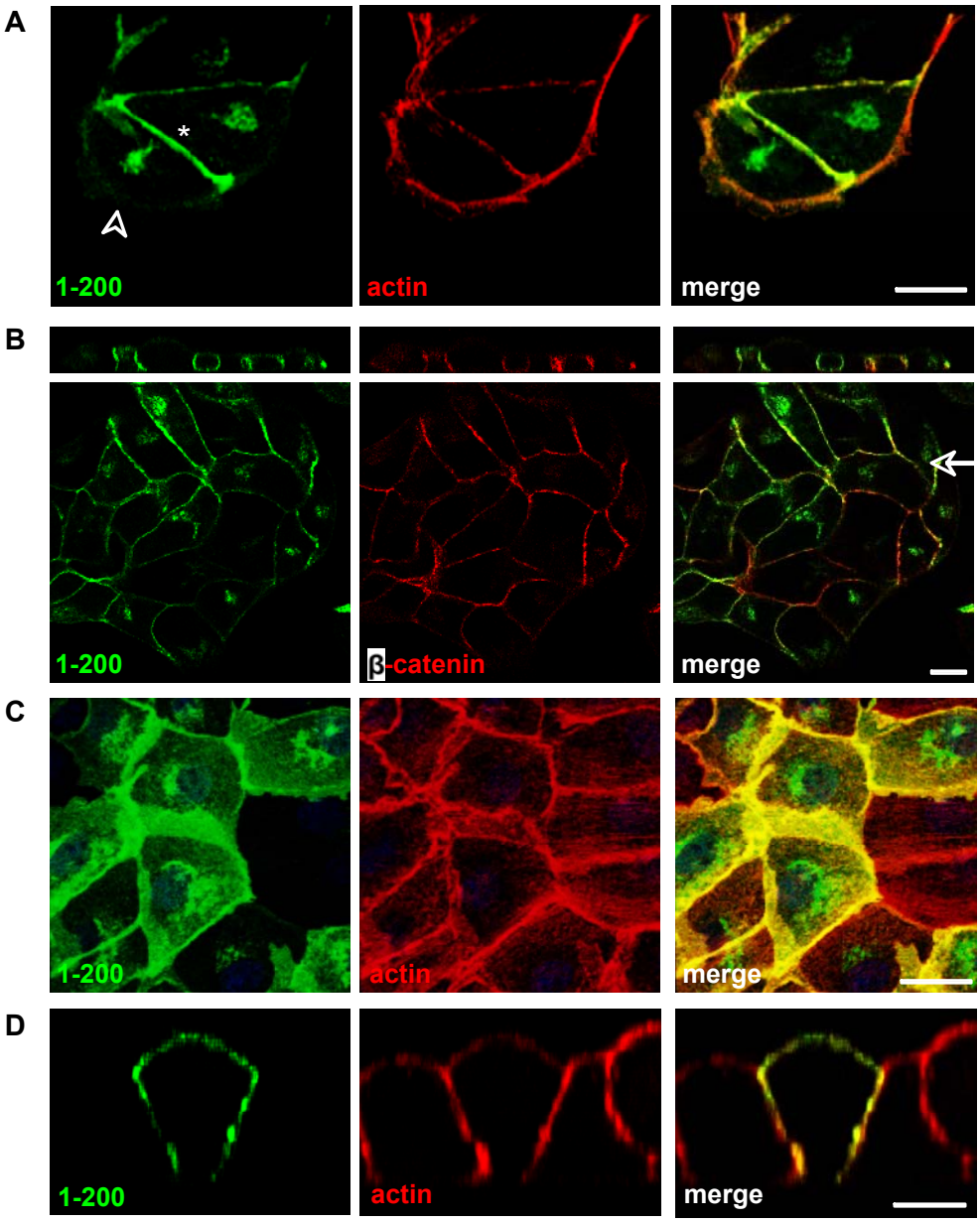

Figure 11: Localisation of CagA 1-200. Confocal microscopy images of GFP CagA 1-200 (green) expressing cells. 3-D reconstructions of confocal z-stacks. Non-polarized cells: A) CagA 1-200 enriched at cell-cell contacts (*), excluded from free edge (➤), actin (red). B) CagA 1-200 co-localization with b-catenin (red) at lateral membrane; (←) z-section of corresponding 3-D reconstruction. C) CagA 1-200 enriched in lamellipodia at cell-cell contacts, actin (red). D) Polarized cells: CagA 1-200 localizes to apical and lateral membrane, actin (red). Bar, 10µm.

3.2.2 CagA mutant lacking the MBD

Having identified the MBD the next step was to delete the MBD from CagA to see what effect it has on CagA localisation. Interestingly, CagA 200-1216 still localises to the membrane albeit to different membrane substructures. This difference is clearly visible in polarised cells (compare Figure 11D and Figure 12B). The CagA 200-1216 mutant distributes equally at the membrane in non-polarized cells even at membrane sites not engaged with cell-cell contacts (see ➤ in Figure Figure 12A), in contrast to the CagA MBD, which is excluded from free edges. In polarized epithelial cells CagA 200-1216 is enriched at the apical membrane (Figure 12B).

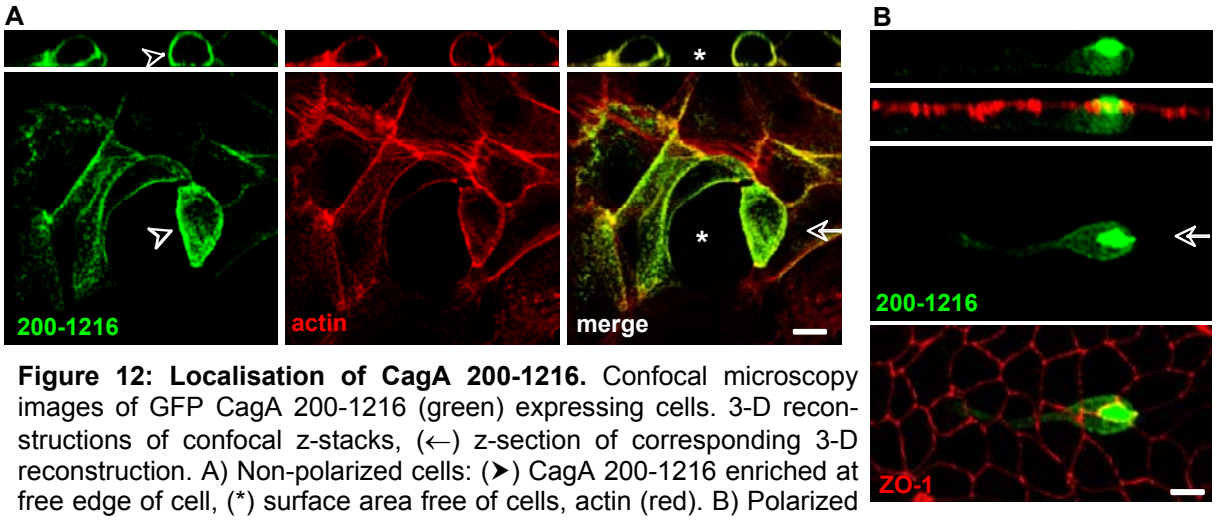

Figure 12: Localisation of CagA 200-1216. Confocal microscopy images of GFP CagA 200-1216 (green) expressing cells. 3-D reconstructions of confocal z-stacks, (←) z-section of corresponding 3-D reconstruction. A) Non-polarized cells: (➤) CagA 200-1216 enriched at free edge of cell, (*) surface area free of cells, actin (red). B) Polarized cells: CagA enriched at apical surface, ZO-1 (red). Bar, 10µm

3.2.3 The localisation of the CagA C-terminus

It has been reported, that the CagA C-terminus (CagA 871-1216) is localised to the cytoplasm (Bagnoli et al., 2005), but another report states that the interaction of CagA with the membrane depends on the EPIYA motif. Since it was established in 3.2.1 that although the MBD is deleted CagA still localises to the membrane, CagA 200-1216 was analyzed in more detail, to determine which part of C-terminal CagA is necessary in order to bind to the membrane. CagA mutants with different amino acid lengths were expressed in polarised epithelial cells and studied via immune fluorescence confocal microscopy. The C-terminal part of CagA 800-1216 is localised in the cytoplasm as well as the segment CagA 200-800. Also the CagA mutant 400-1216 is localised to the cytoplasm, indicating that the whole part 200-1216 of CagA is necessary to localise it to the membrane (Figure 13).

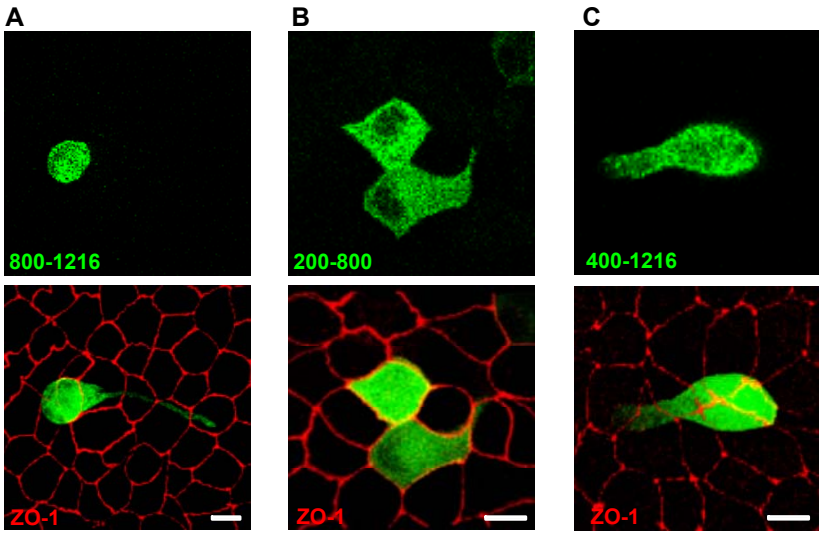

Figure 13: CagA mutants localise in the cytoplasm. Confocal microscopy images of mutant GFP-CagA (green) expressing cells. Upper panel: x-y plane, lower panel: 3-D reconstructions of confocal z-stacks. Polarized cells A) CagA 800-1216 B) CagA 200-800 C) CagA 400-1216 are all localised to the cytoplasm.

A cytoplasmic IF signal can mask a membrane associated signal, therefore the distribution of CagA 800-1216, 200-800 and 200-1216 between membrane and cytoplasm was analyzed in a membrane-pelleting assay. Approximately two thirds of the CagA 800-1216 mutant protein can be detected in the membrane fraction and the high-speed centrifugation step also revealed that roughly half of the mutant protein CagA 200-800 associates with the membrane compartment (Figure 14). These data reveal that the EPIYA containing C-terminus can interact with membrane fractions, but is not sufficient for complete membrane attachment in epithelial cells.

The membrane-pelleting assay furthermore confirmed that CagA 200-1216 is entirely localised to the membrane (Figure 14), demonstrating that a very large segment of the C-terminal CagA protein is required for complete membrane attachment.

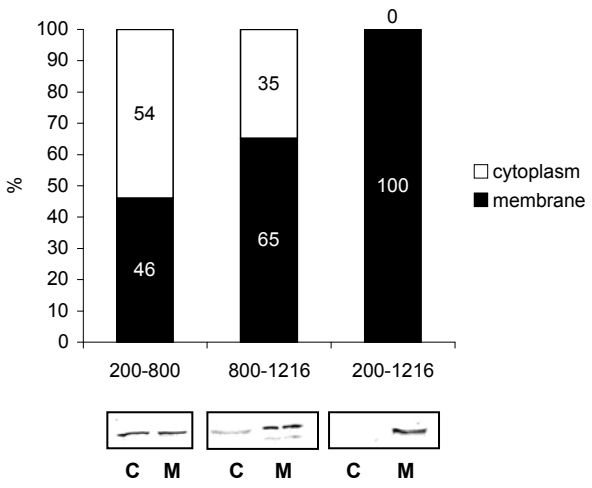

Figure 14: Membrane-pelleting assay. Signal intensity for each protein band was determined as integrated intensity (counts/mm^2) and expressed as percentage of the sum of integrated intensities in M (membrane) and C (cytoplasm).

3.2.4 CagA expression in trans

Previously, it has been shown that CagA 1-877 and CagA 871-1216 can interact with each other when ectopically expressed in trans (Bagnoli et al., 2005) and thereby CagA 871-1216 is targeted to the membrane. Since membrane targeting is important for many effects of CagA on host cell biology, the ability of CagA localisation to the membrane was further investigated.

Different CagA mutants were transiently expressed in a stable cell line expressing CagA 871-1216. The interaction of CagA mutants with CagA 871-1216 was investigated. CagA 200-800 can interact with CagA 871-1216 and localise it to the membrane (Figure 15A).

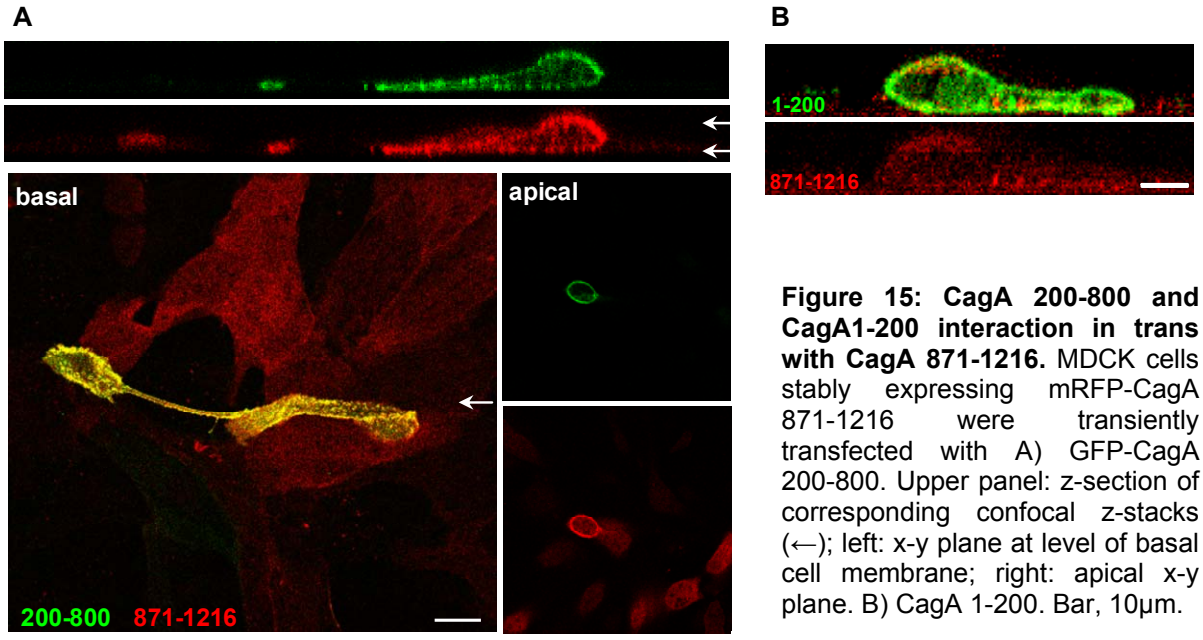

Figure 15: CagA 200-800 and CagA1-200 interaction in trans with CagA 871-1216. MDCK cells stably expressing mRFP-CagA 871-1216 were transiently transfected with A) GFP-CagA 200-800. Upper panel: z-section of corresponding confocal z-stacks (←); left: x-y plane at level of basal cell membrane; right: apical x-y plane. B) CagA 1-200. Bar, 10µm.

In contrast CagA 1-200 is not able to interact with CagA 871-1216. CagA 1-200 is localised to the membrane whereas CagA 871-1216 is localised to the cytoplasm (Figure 15B).

However, membrane attachment may be necessary for certain effects of the CagA C-terminus. When expressed as a fusion protein (CagAΔ200-800) the MBD delivers CagA 800-1216 to the membrane (Figure 16). There is now a tool to look at effects of

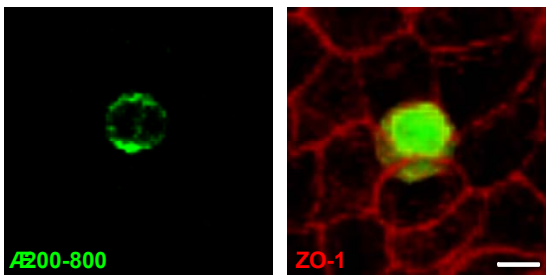

Figure 16: Cellular distribution of CagA Δ200-800 mutant. right image: 3-D reconstruction of confocal z-stacks, left image: representative x-y plane. GFP-CagA Δ200-800 (green), actin (red). Bar, 10µm.

CagA C-terminus, which may need a complete localisation to the membrane.

The CagA constructs have been verified for their correct expression by immunoblotting. In Figure 17 CagA wt, CagA 200-1216, CagA 200-800, CagA ∆200-800 and CagA 400-1216 are shown. CagA 1-200. CagA 25-225 and CagA 1-150 are shown in Figure 10. The CagA construct 800-1216 is shown in Figure 21.

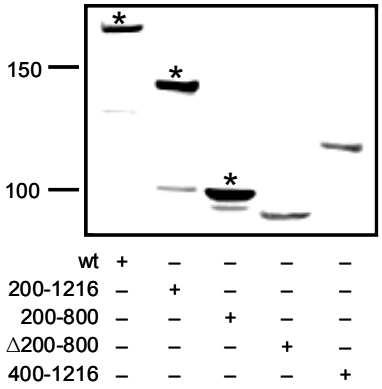

Figure 17: Immunoblot of CagA wt/CagA mutants. (*) indicates specific band in lanes 1-3. Size difference between CagA 200-800 and Δ200-800 is due to additional SBP/CBP tag in CagA 200-800.

3.3 Functional analysis of CagA MBD

3.3.1 Constriction of apical surface in polarized epithelial cells

Following identification of the MBD and the C-terminal binding sequence of CagA, the question arose if there was any interference with each other's effects on host cell biology. Whereas CagA 1-200 localizes along the apical and lateral membrane in polarized epithelia, CagA 200-1216 is enriched at the apical site. Strong apical localisation of CagA 200-1216 raised the question of whether or not it actually enhances constriction of apical membrane surfaces characteristic for the migratory phenotype. CagA wt significantly reduces the apical surface area compared to non-expressing control cells (Median 102 vs. 198.5; Figure 18B). Expression of the CagA 200-1216 mutant further reduces the apical surface area compared to wild type CagA (Median 40). The subcellular localisation to the apical membrane and phosphorylation of the EPIYA C motifs are important here, as CagA 400-1216 and CagA EPISA C mutants do not constrict the apical surface, respectively (Figure 18A, B). CagA 1-200 has no effect on apical constriction (Figure 11D). These data suggest that CagA 1-200 interferes with CagA 200-1216 mediated constriction of the apical surface area by way of targeting CagA wt to a different membrane structure in polarized epithelia.

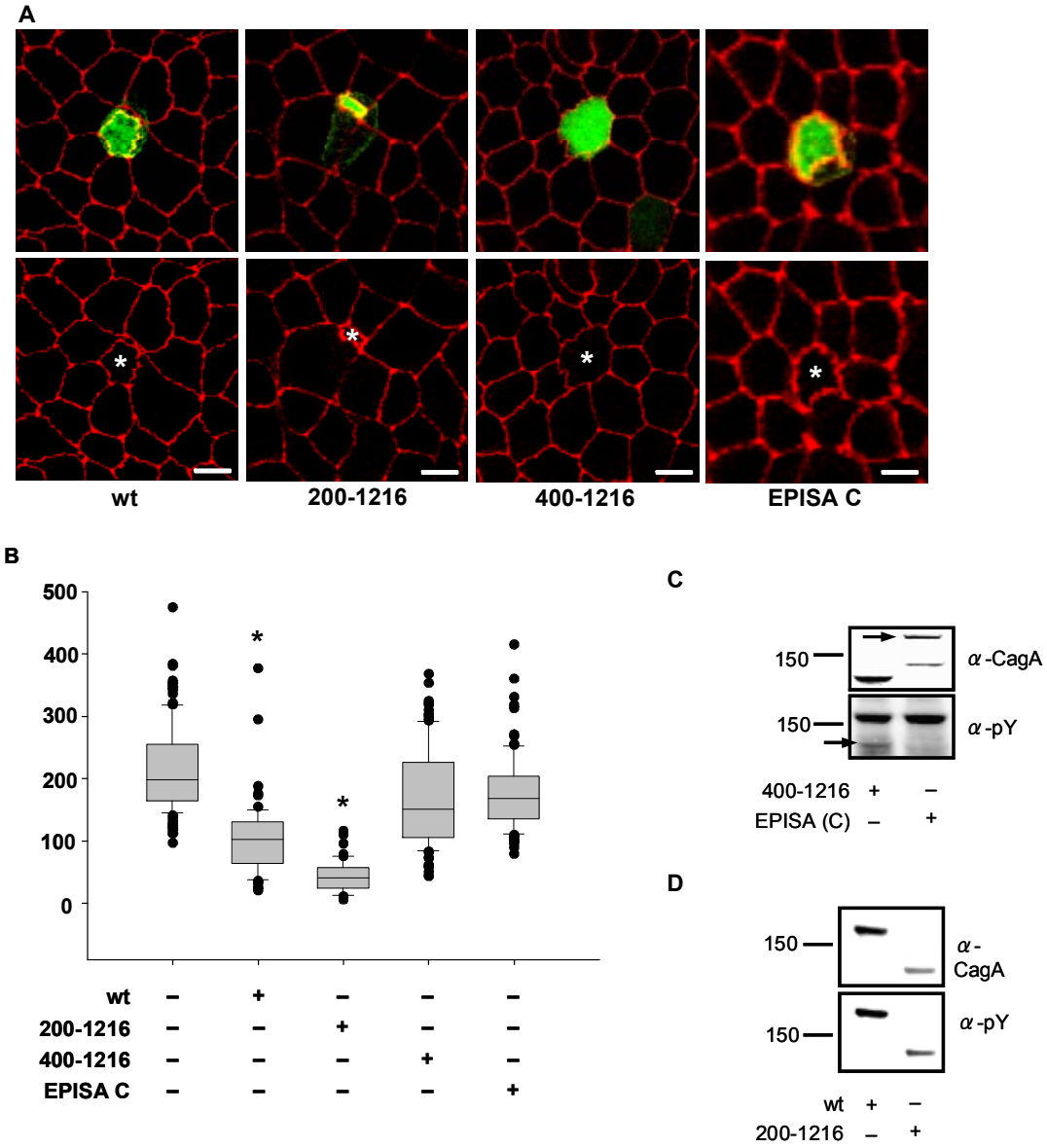

Figure 18: Apical constriction of CagA mutants. A) 3-D reconstructions of confocal z-stacks, (*) indicates apical surface area of CagA expressing cells. GFP-CagA wt and GFP-CagA mutants (green), ZO-1 (red). B) Box plot graph of apical surface area. Control n=136, wt n=64, 200-1216 n=86, 400-1216 n=92, EPISA C n=100 cells. (*) p<0.0001 (Wilcoxon Signed Rank Test). C and D) Immunoblot of CagA wt, 200-1216, 400-1216 and EPISA C mutants and respective tyrosine phosphorylation, (→) indicate specific bands.

3.3.2 Elongation

3.3.2.1 CagA MBD inhibits migratory phenotype

One characteristic phenotype for CagA is the formation of cellular protrusions, which is also an aspect of the migratory phenotype. The number of cells with cellular protrusions extending the diameter of the cell body were counted in transiently transfected polarized MDCK cells. CagA wt expressing cells develop cellular protrusions in 24.7% +/- 4% of CagA transfected cells. The formation of cellular protrusions is

significantly increased to 41.1% +/- 8% in CagA 200-1216 mutant cells (Figure 19). This suggests that the CagA MBD attenuates the formation of cellular protrusions.
CagA 800-1216 induces cellular protrusions similar to CagA 200-1216 (46% +/- 3.3%), which suggests that weaker membrane interaction has no impact on cell elongation (Figure 19).

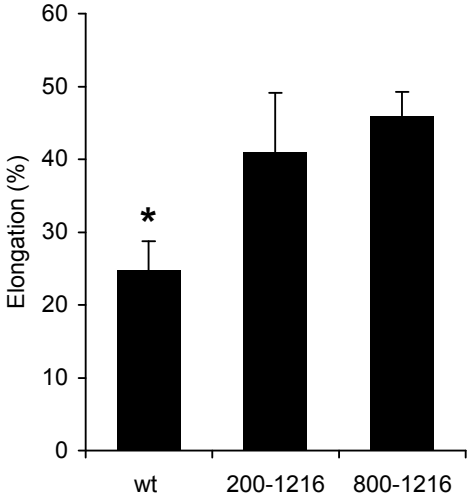

Figure 19: Elongation of CagA expressing cells. Percentage of elongated cells transiently transfected with CagA wt or CagA mutants in polarized epithelia; data are presented as mean ± S.E.M.; (*) p<0.0001, (Cochran–Mantel–Haenszel Test); number of cells (n) counted in 6 independent experiments CagA wt n=785, CagA 200-1216 n=747, CagA800-1216 n=1024.

In order to test if CagA 1-200 inhibits cell signalling mediated by the C-terminus of CagA, a CagA mutant was constructed lacking AA 200-800, the domain necessary for apical membrane targeting (CagA Δ200-800). CagA 1-200 targets the C-terminus of CagA (CagA 800-1216) to the cell membrane in this mutant (see Figure 16). CagA 1-200 itself has no effect on cell elongation. Epithelial cells expressing CagA Δ200-800 elongate in 24.4% +/- 5.8% of transfected cells similar to CagA wt (Figure 20).

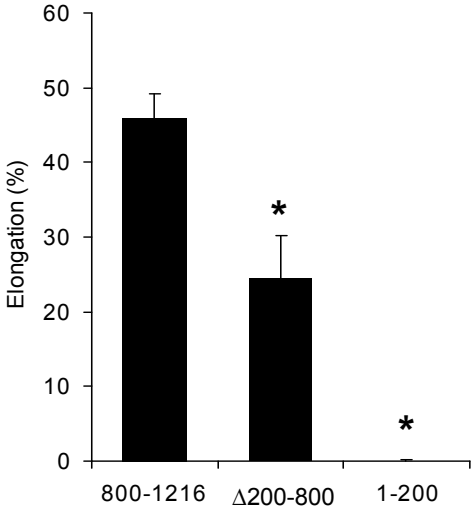

Figure 20: CagA 1-200 inhibits elongation. Percentage of elongated cells transiently transfected with CagA mutants in polarized epithelia; data are presented as mean ± S.E.M.; (*) p<0.0001, (Cochran–Mantel–Haenszel Test); number of cells (n) counted in 6 independent experiments CagA800-1216 n=1024, CagAΔ200-800 n=873, CagA1-200 n=612.

These data suggest that the CagA 1-200 MBD inhibits the effects of the CagA C-

terminus by targeting EPIYA and CM/CRIPA motifs to an alternative membrane compartment.

3.3.2.2 Formation of cellular protrusions depends on EPIYA and CM/CRPIA motifs

The formation of cellular protrusions depends on EPIYA and CM/CRPIA motifs. CagA 800-1216EPISA C, a mutant, which can only be phosphorylated at EPIYA motifs A and B, shows significantly less elongation (21.4% +/- 6.3%) compared to CagA 800-1216 (32.3% +/- 1.4%). The deletion of all CM/CRPIA and EPIYA C motifs in CagA 800-1216ΔPar1 abolishes cell elongation (3% +/- 3.2%) despite the remaining phosphorylation sites EPIYA A and B suggesting that both motifs are required for a complete elongation phenotype. A CagA 800-1216$_{EPISA}$ mutant that has the tyrosine residues mutated to serine in the EPIYA motifs A and B and the EPIYA C region deleted cannot be phosphorylated but still elongates polarized epithelial cells (27.9% +/- 5,9%) (Figure 21A). In contrast to the deletion mutant in CagA 800-1216ΔPar1, the first CM/CRPIA motif is preserved in CagA 800-1216$_{EPISA}$. This demonstrates that CM/CRPIA induced signalling elongates cells independent of EPIYA phosphorylation.

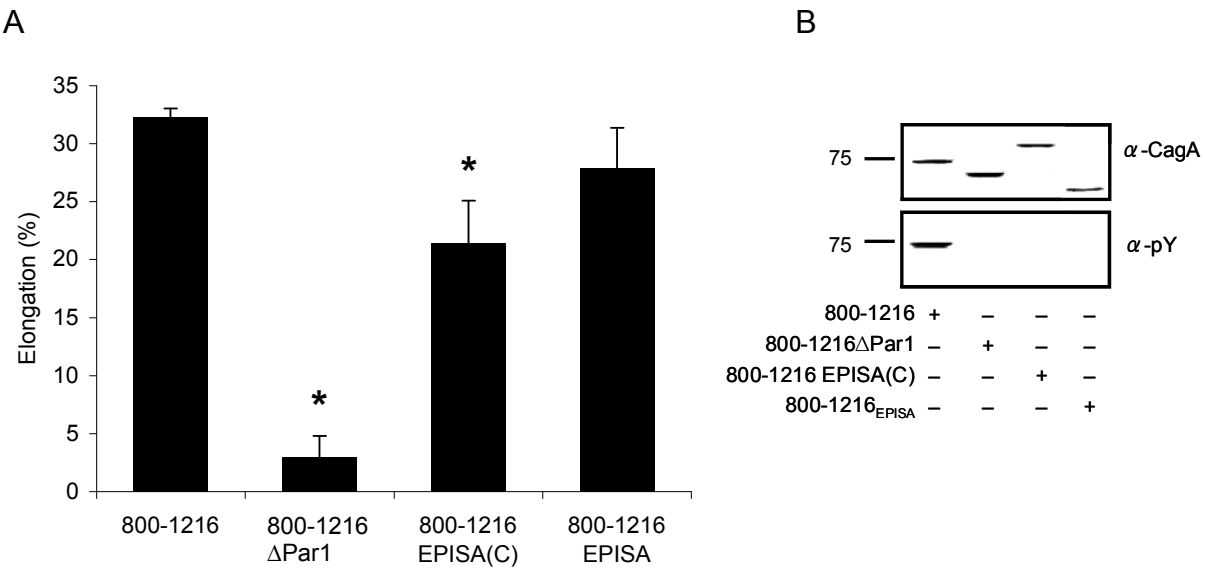

Figure 21: CagA 800-1216 mutants. Percent of elongated cells transiently transfected with CagA mutants in polarized epithelia; data are presented as mean ± S.E.M.; (*) p<0.0001, (Cochran–Mantel–Haenszel Test); number of cells (n) counted in 3 independent experiments CagA 800-1216 n=748, 800-1216ΔPar1 n=544, 800-1216EPISA (C) n=654, 800-1216$_{EPISA}$. B) Immunoblot of CagA 800-1216 mutants and respective tyrosine phosphorylation. Size difference between CagA 800-1216 and 800-1216 EPISA C is due to additional SBP/CBP tag in CagA 800-1216 EPISA C. CagA 800-1216 ΔPar1, 800-1216 EPISA C and EPISA C mutants are not phosphorylated despite presence of EPIYA A and B motifs. One explanation would be that the immunoblot is not sensitive enough to detect the low amounts of phosphorylated EPIYA A B motifs. Another explanation could also be that the EPIYA A B motifs are not phosphorylated at all. There is a report saying that only two EPIYA motifs are phosphorylated in the H. pylori G27 strain (Backert et. al 2001).

To test if the dependency of the elongation phenotype on the CM/CRIPYA and EPIYA motif is also true for wild type CagA and for CagA 200-1216, the protrusions of the constructs ΔPar1, EPISA(C), 200-1216 ΔPar1, 200-1216 EPISA (C) and 200-1216 EPISA were counted and summarised in Figure 22. The same tendency can be observed as for the CagA 800-1216 mutant constructs. CagA EPISA (C) and CagA 200-1216 EPISA (C) show less elongation compared to CagA wt and CagA 200-1216 respectively. Deletion of all CM/CRPIA and EPIYA C motifs abolishes cell elongation. Additionally, a CagA 200-1216_{EPISA} mutant still elongates polarized epithelial cells.

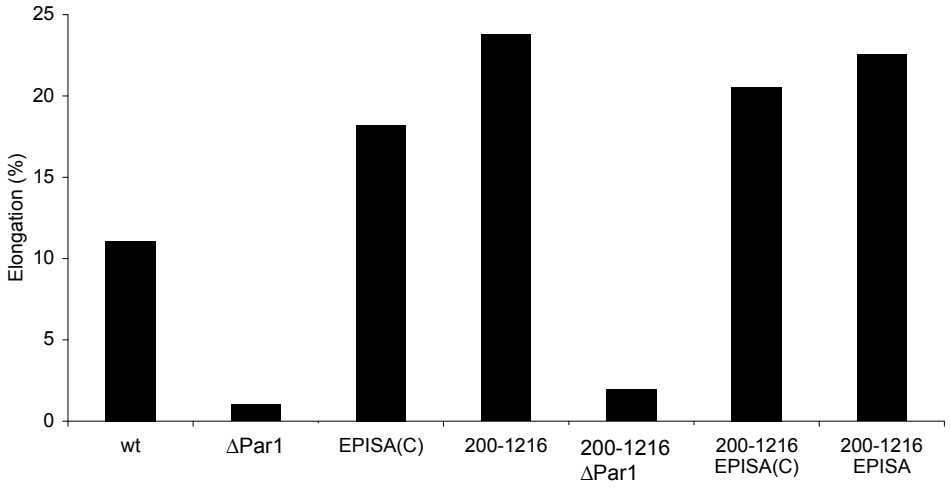

Figure 22: Elongation of various CagA mutants. Percentage of elongated cells transiently transfected with CagA mutants in polarized epithelia; number of cells counted 185 ± 51.

3.3.3 CagA MBD inhibits transcriptional activity of b-catenin

Adherens junctions mediate cell-cell adhesion. The trans-membrane protein E-cadherin is an important component of adherens junctions and binds directly to β-catenin. This interaction is stabilized when cell-cell contacts are established (Nelson, 2008). A different role of β-catenin is its function as a transcriptional regulator of gene expression in the nucleus by binding to T-cell factor (TCF)/lymphoid enhancer factor (LEF) transcription factors (Nelson and Nusse, 2004). CagA has been described as causing a disruption to the E-cadherin/β-catenin complex leading to a weakening of cell-cell adhesion and to an increase of transcriptional activity of β-catenin (Franco et al., 2005; Murata-Kamiya et al., 2007; Suzuki et al., 2005). CagA induced increase in TCF/β-catenin transcriptional activity, which is mediated by the CM/CRPIA motif in

the C-terminus of CagA (Suzuki et al., 2009), has been shown in cell lines with a constitutive TCF/β-catenin transcriptional activity (Franco et al., 2005; Murata-Kamiya et al., 2007). In the MDCK cell model used in this work, TCF/β-catenin mediated transcription is not constitutively activated (Barth et al., 1997) and CagA wt does not alter TCF/β-catenin transcriptional activity (Figure 23)

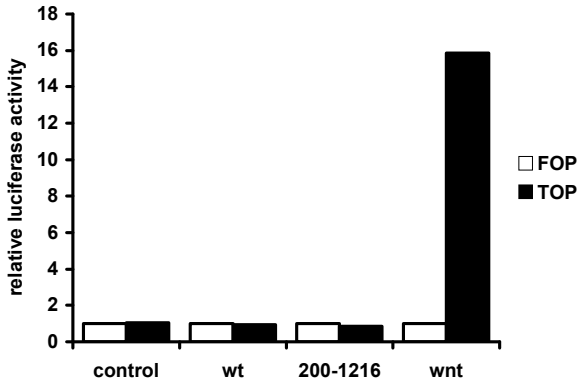

Figure 23: No increase of TCF/β-catenin transcriptional activity in MDCK cells. TCF/β-catenin transcriptional activity of MDCK cells transiently transfected with CagA wt, CagA 200-1216, wnt or empty vector. TOPflash (black), FOPflash (white)

Therefore, the gastric epithelial cell line NCI-N87, which forms adherens junctions and has constitutive TCF/β-catenin transcriptional activity (Caca et al., 1999; Yokozaki, 2000) was used for testing effects of the CagA 1-200 MBD on β-catenin transcriptional activity in a gastric epithelial cell. The baseline transcriptional activity of β-catenin is increased in these cells (compare TOP to FOP in control cells; Figure 24). The CRPIA containing CagA mutant 200-1216 increases TOP luciferase activity as a measure for β-catenin transcriptional activity by 2.65-fold to control cells ($p<0.0001$). Consistent with its stimulating effect on cell-cell adhesion, the CagA 1-200 MBD attenuates CagA 200-1216 induced β-catenin transcriptional activity by 27% as CagA wt induced TOP luciferase activity is only 1.93-fold compared to control ($p<0.0001$).

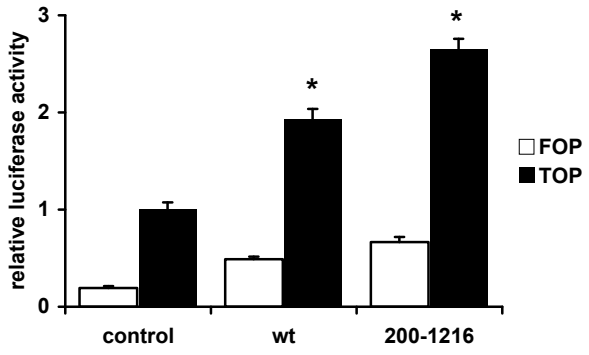

Figure 24: CagA MBD decreases TCF/b-catenin transcriptional activity. TCF/β-catenin transcriptional activity of NCI-N87 cells transiently transfected with CagA wt, CagA 200-1216 or empty vector. Data represent mean ± S.E.M. calculated from three independent experiments as x-fold induction compared to activity of reporter vector in the absence of CagA (*) $p<0.0001$ (One-way ANOVA; Tukey's Multiple Comparison Test). TOPflash (black), FOPflash (white).

3.3.4 CagA 1-200 membrane-binding domain increases cell-cell adhesion

The CagA induced migratory phenotype in polarized epithelial cells is characterised by reduced cell-cell adhesion when CagA expressing cells become migratory and detach from neighbouring cells (Bagnoli et al., 2005). To examine the effects of CagA 1-200 domain on cell-cell adhesion a functional cell-cell adhesion assay was performed. This assay determines the size of cell clusters formed over time from single cells in suspension. Applying shearing forces through trituration reveals also the strength of newly formed adhesion complexes (Ehrlich et al., 2002). The MDCK cells stably and inducible expressing CagA or CagA mutants used for this assay had comparable expression levels and are expressed in about 90% of cells (Figure 25).

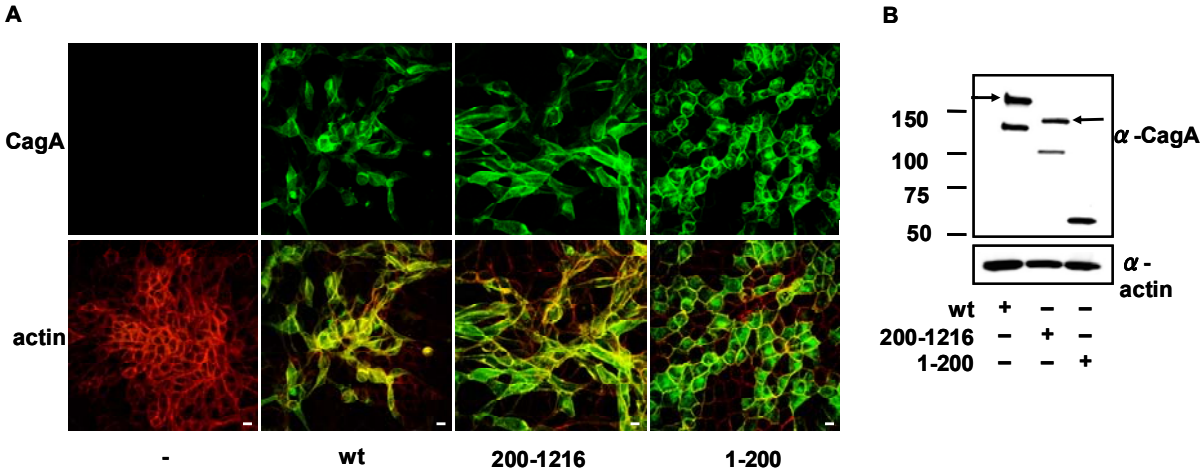

Figure 25: MDCK cell clones stably expressing CagA wt/CagA mutants. MDCK cell clones stably expressing GFP-CagA wt, 200-1216 and 1-200 in Tet-On inducible system. A) Confocal microscopy images: 3-D reconstructions of confocal z-stacks. GFP-CagA (green), actin (red). Control: non-induced representative clone. Bar, 10µm. B) Immunoblot of CagA wt/CagA mutants show similar expression levels of CagA. (→) indicate specific bands.

Experiments were performed in triplicates with 200-400 cells examined at each time point in each experiment using non-induced cells as control. First clusters were counted without trituration after 2 hours and 4 hours.

In control cells, 28% of clusters consist of more then 10 cells/cluster after 2 hours and 62% after 4 hours (sum of grey and black area). Cluster formation with more then 10 cells/cluster in CagA wt expressing cells is not significantly different to control after 4 hours (57%), but significantly decreased to 39% in CagA 200-1216 mutant cells. Surprisingly, expression of the CagA 1-200 MBD increases the rate of cell cluster formation to 53% after 2 hours and 100% of clusters with 10 or more cells after 4 hours (Figure 26).

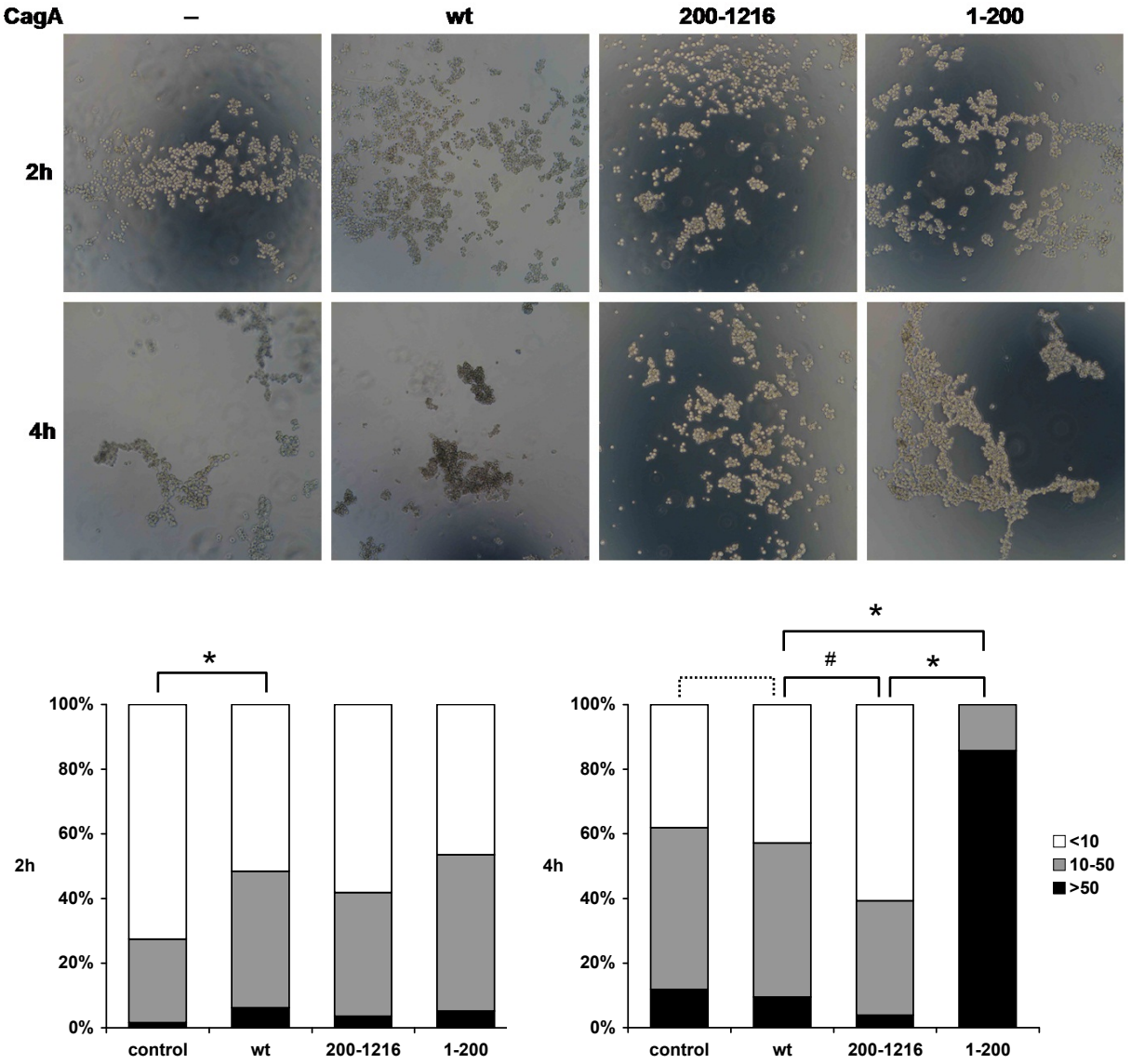

Figure 26: Quantitative, functional adhesion assay - Before Trituration. MDCK cells stably expressing CagA wt, 200-1216 and 1-200 mutants (induced by doxycycline 24h before experiments). Control represents pooled data from non-induced MDCK cells of all three clones. At each time point three drops were photographed, and numbers and sizes of clusters were determined. Graphs show percentage of cells in clusters of 0–10 cells (white), 11–50 cells (gray), and >50 cells (black) at the time points indicated before trituration. For each time point, 200–400 cells were scored and data are presented as the average of three independent experiments; (…) not significant, (*) $p<0.0001$, (#) $p<0.05$ (Cochran–Mantel–Haenszel Test). Photographs are representative fields at 2 and 4 h before trituration.

The application of shearing forces revealed that the CagA 1-200 domain also increases the strength of cell-cell adhesion in formed cell clusters (Figure 27). After trituration of cell clusters formed after 4 hours, the number of large cell clusters (10-50 and >50 cells/cluster group) is similar between CagA wt and control cells and significantly increased in CagA 1-200 expressing cells (52% vs. 54% vs. 70%, respectively). Epithelial cells expressing the CagA 200-1216 mutant form dramatically weaker cell-cell adhesions after 2 and 4 hours (11% and 9% of clusters

with more then 10 cells, respectively). These data show that the CagA C-terminus MBD 200-1216 mediates loss of cell-cell adhesion and CagA 1-200 counteracts this effect by increasing cell-cell adhesion formation.

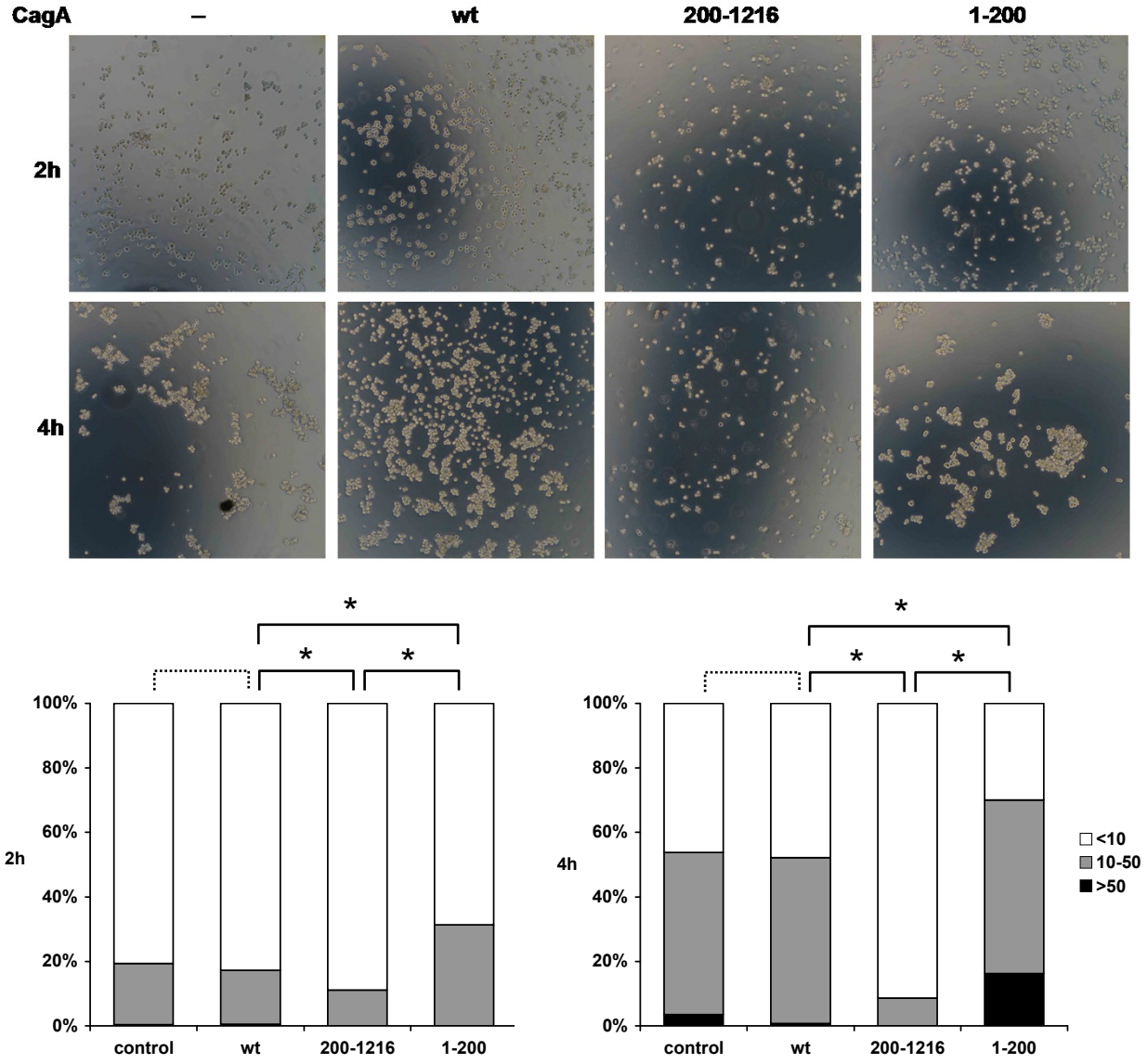

Figure 27: Quantitative, functional adhesion assay - After Trituration. MDCK cells stably expressing CagA wt, 200-1216 and 1-200 mutants (induced by doxycycline 24h before experiments). Control represents pooled data from non-induced MDCK cells of all three clones. At each time point three drops were triturated, photographed, and numbers and sizes of clusters were determined. Graphs show percentage of cells in clusters of 0–10 cells (white), 11–50 cells (gray), and >50 cells (black) at the time points indicated after trituration. For each time point, 200–400 cells were scored and data are presented as the average of three independent experiments; (…) not significant, (*) $p<0.0001$, (#) $p<0.05$ (Cochran–Mantel–Haenszel Test). Photographs are representative fields at 2 and 4 h after trituration.

3.3.5 Loss of epithelial barrier function of CagA expressing cells

It has been described, that CagA disrupts the barrier function of polarised epithelial cells, which results in an altered flux of ions (Amieva et al., 2003). This can be evaluated by measuring the transepithelial electrical resistant (TER) of epithelial monolayers.

It was shown in 3.3.2 that targeting CagA to different membrane substructures could attenuate the CagA induced hummingbird phenotype. Furthermore deleting the MBD in 3.3.1 leads to an increase of apical constriction, which is a characteristic for the migratory phenotype. In addition in 3.3.4 it was shown that the MBD leads to an increase of cell adhesion.

Subsequently, the question arose if the MBD plays a role in tight junction formation, hence epithelial barrier function. The MBD could lead to an increased barrier function and accordingly, deleting the MBD should lead to a more pronounced barrier defect.

For the following experiments MDCK cells stably expressing CagA and CagA mutants were used. Since the TER is a very sensible parameter the inducible gene expression system has the great advantage that effects in TER can exclusively be attributed to CagA expression.

When MDCK cells are seeded at high density on Transwell filters they start to polarize within 6 hours. After 21 hours they reach their maximum TER, which stays constant for at least three days (Figure 28).

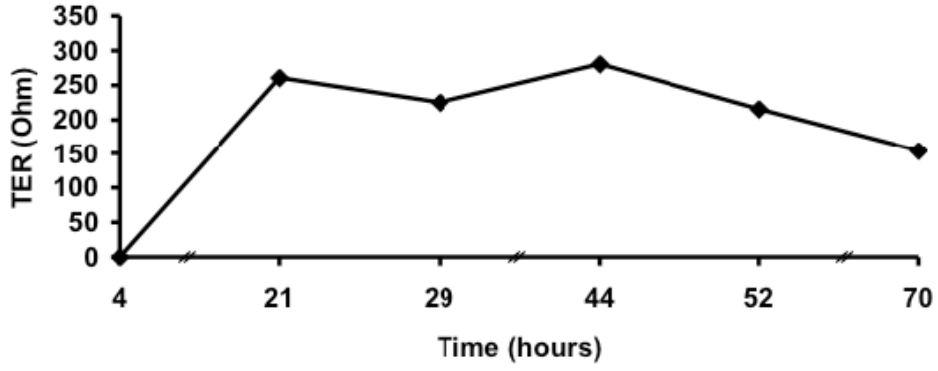

Figure 28: TER of MDCK. After 21 hours TER is at maximum and stays constant for at least three days.

The TER of CagA stable cell lines was measured during epithelial barrier formation. Approximately 21 hours after seeding, monolayers of uninduced stable cell lines reach the maximum TER. This time point was chosen to compare TER values between CagA expressing cell lines. Since the stable cell lines do not have the equal basal TER values the percentage loss of TER was calculated and summarized in Figure 29H. P-values were calculated compared to the Teton cell line expressing the Trans-activator (Figure 29A). Consistent with published data, expression of CagA wt significantly reduced TER (-269 ohm ± 21 ohm, $p<0.0001$) during barrier formation, but 39 hours after seeding, the full barrier function is reached (Figure 29B). The next question to address was, if the MBD could elevate epithelial barrier formation. Surprisingly the MBD (CagA 1-200) did not alter the barrier formation (-12 ohm ± 10 ohm) (Figure 29E). The MBD deletion mutant CagA 200-1216 also had a delayed barrier formation as observed for CagA wt (-148 ohm ± 16 ohm $p<0.001$), but it failed to elevate the barrier formation defect (Figure 29C). Consistent with the results of CagA wt and CagA 200-1216 tight junction formation was also delayed for the CagA mutant 800-1216 (-169 ohm ± 27 ohm $p<0.001$) (Figure 29F). As shown for the MBD the CagA mutant 1-800 didn't have an effect on the barrier formation (32 ohm ± 19 ohm) (Figure 29G).

Next, it was tested if targeting of CagA 800-1216 to a different membrane structure through the MBD, leads to an attenuated barrier formation defect as observed for the formation of protrusions in 3.3.2, which was significantly reduced when the CagA C-terminus was localised to a different membrane compartment. Targeting CagA Δ200-800 to different membrane structures did not attenuate the barrier formation defect. CagA Δ200-800 displayed a severe barrier formation defect (-132 ohm ± 14 ohm, $p<0.001$) as CagA wt and all other CagA constructs containing the C- terminal part of CagA did (Figure 29D).

In conclusion the barrier formation defect is constrained to the C-terminus. Figure 29H shows that all cell lines expressing the C-terminal part of CagA display a barrier formation defect with relatively equal levels of reduced TER. The MBD has no influence on the tight junction and epithelial barrier formation of polarised cells. When the C-terminal part of CagA containing the EPIYA and CM/CRIPYA domains is present the formation of the barrier function is delayed.

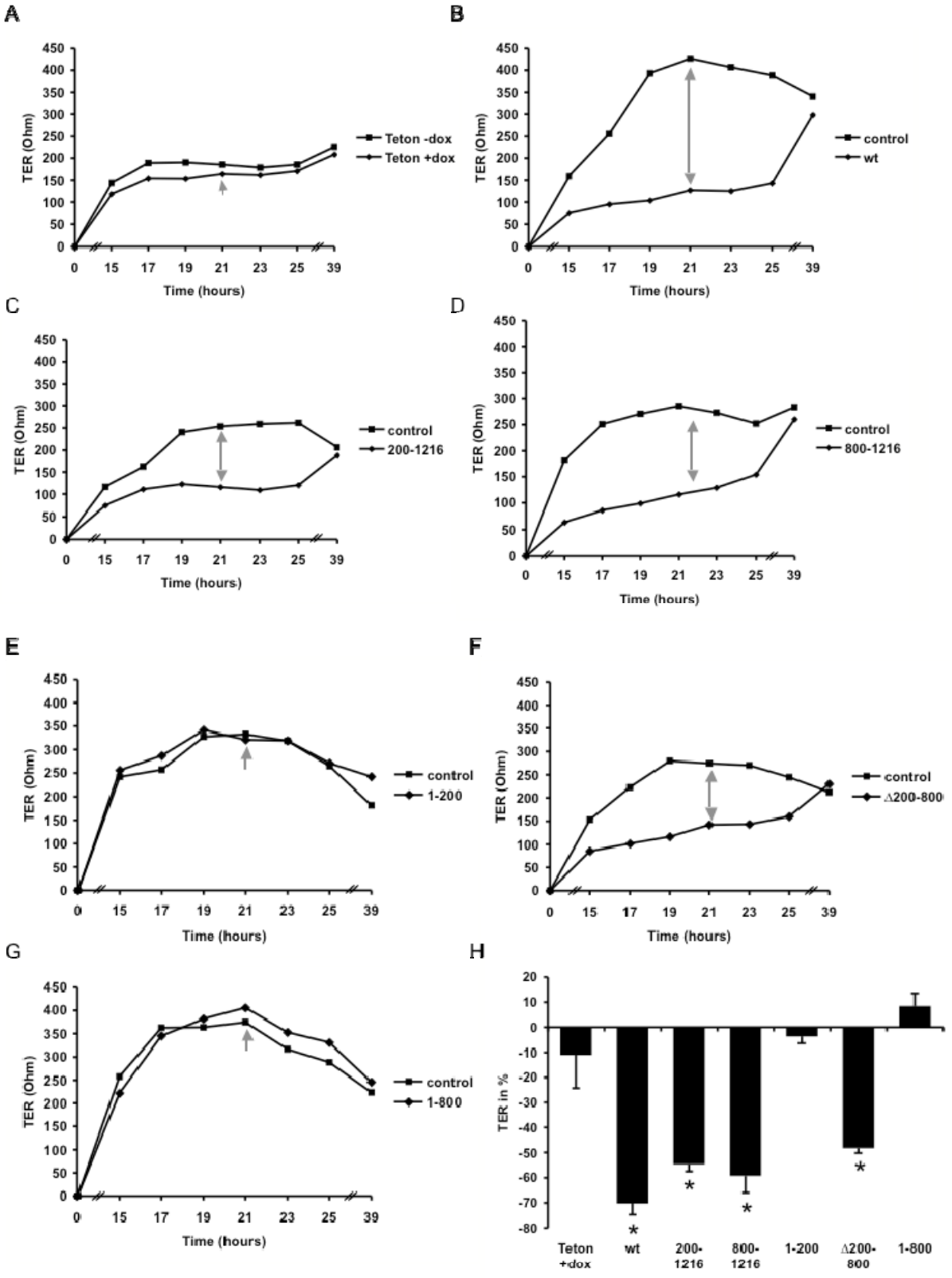

Figure 29: CagA leads to a barrier formation defect of epithelial monolayers. A) Teton stable cell line with and w/o dox showing no effect of dox on barrier formation. B-G) TER of stable cell lines expressing CagA FL, 200-1216, CT, 1-200, Δ200-800 and NT vs. control. CagA cell lines expressing the C-terminal part of CagA show a barrier formation defect. Arrow: 21 hours after seeding H) Difference in TER values of CagA and mutant CagA monolayers shown in A-G at 21 hours after seeding. TER is significantly reduced in CagA cell lines expressing the C-terminal part of CagA compared to Teton. asterisk = $p<0.01$ (ANOVA; Dunnett Multiple Comparisons Test)

The experiments on TER have so far illustrated that the barrier formation defect was strictly restricted to the C-terminus of CagA. Targeting CagA to different substructures did not enhance or reverse barrier formation defects induced by CagA. Saadat et.al showed that CagA induced disruption of the barrier function is reversible by co-expression of Par1b, a protein that interacts with CagA through the CM/CRIPYA motif (Saadat et al., 2007).

For that reason stable cell lines expressing CagA ΔPar1 and CagA 800-1216 ΔPar1 were analysed for defects in barrier formation. The CagA in these cell lines has deleted CM/CRIPYA motifs. At 21 hours after seeding, no defect in the formation of the barrier function could be detected (CagA wt -190 ohm ± 50 ohm vs. CagAΔPar1 34 ohm ± 12 ohm) and (CagA 800-1216: -294 ohm ± 15 ohm vs. CagA800-1216ΔPar1: 16 ohm ± 9 ohm) (Figure 30). This result strongly suggests that the CM/CRIPYA motif is indeed involved in the barrier formation defect, most likely through interaction with Par1b.

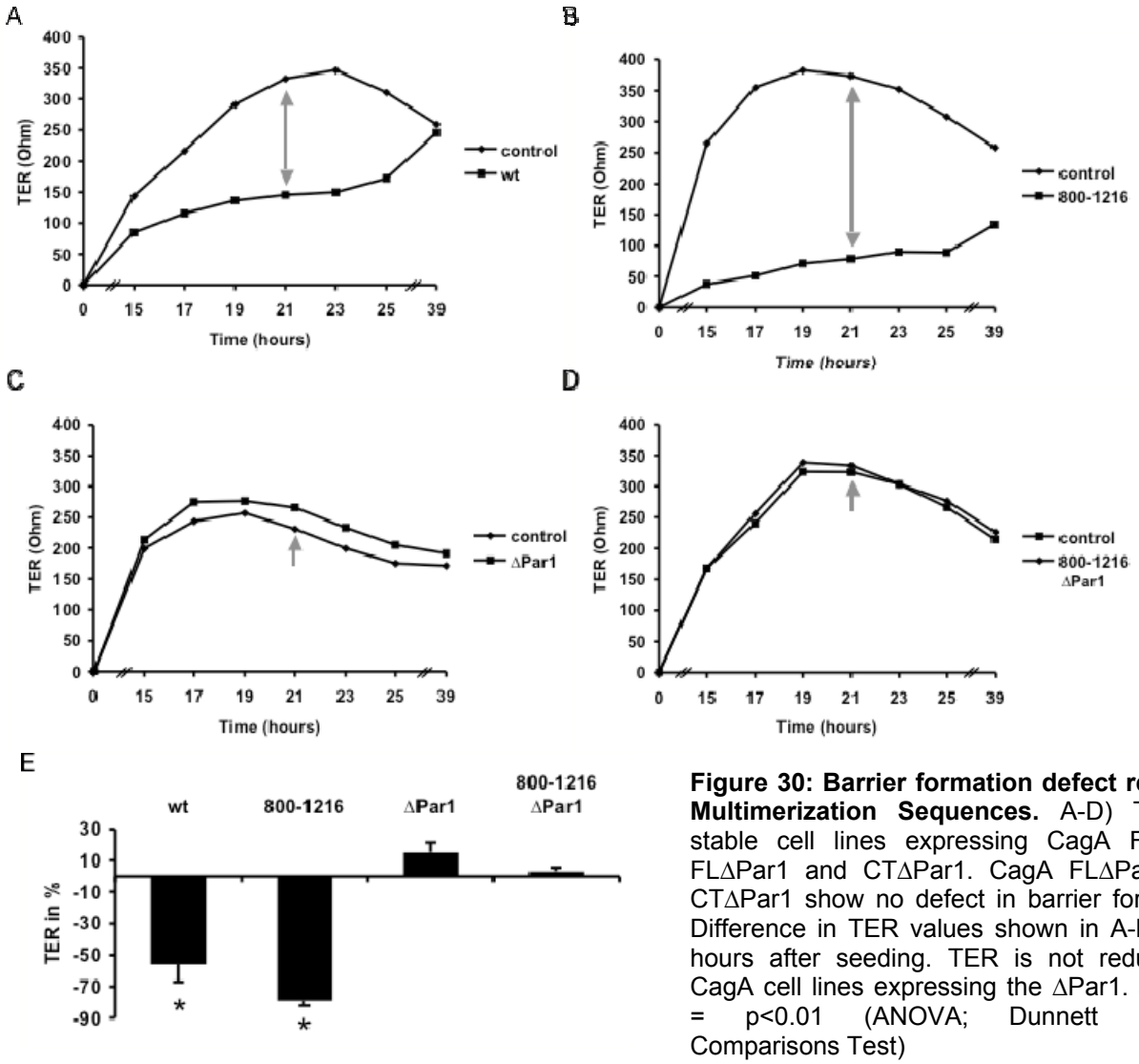

Figure 30: Barrier formation defect requires Multimerization Sequences. A-D) TER of stable cell lines expressing CagA FL, CT, FLΔPar1 and CTΔPar1. CagA FLΔPar1 and CTΔPar1 show no defect in barrier formation. Difference in TER values shown in A-D at 21 hours after seeding. TER is not reduced in CagA cell lines expressing the ΔPar1. asterisk = $p<0.01$ (ANOVA; Dunnett Multiple Comparisons Test)

3.3.6 3D-Cell Culture

Three-dimensional (3D) epithelial culture systems allow epithelial cells to organise into structures that resemble their in vivo structure. Additionally, 3D culture models have two advantages that distinguish them from 2D cell culture, mouse models or human tissues. Firstly, they are readily accessible for manipulation and microscopic analysis and secondly they recapitulate certain essential structural features of glandular epithelium in vivo. Figure 31 shows a model of the formation of cysts (From Debnath and Brugge, 2005). MDCK cells form cysts after 7-10 days when grown on collagen gels with a lumen at the inside of the cysts, the apical membrane facing inwards towards the lumen and the basal-lateral membranes facing outwards (Pollack et al., 1997). A variation of this technique is to use laminin-rich basement membrane material from Englebreth-Holm Swarm tumors (matrigel) instead of collagen type I (Muthuswamy et al., 2001). Matrigel is a more physiological basement membrane material and contains growth factors, which may have an influence on cyst formation.

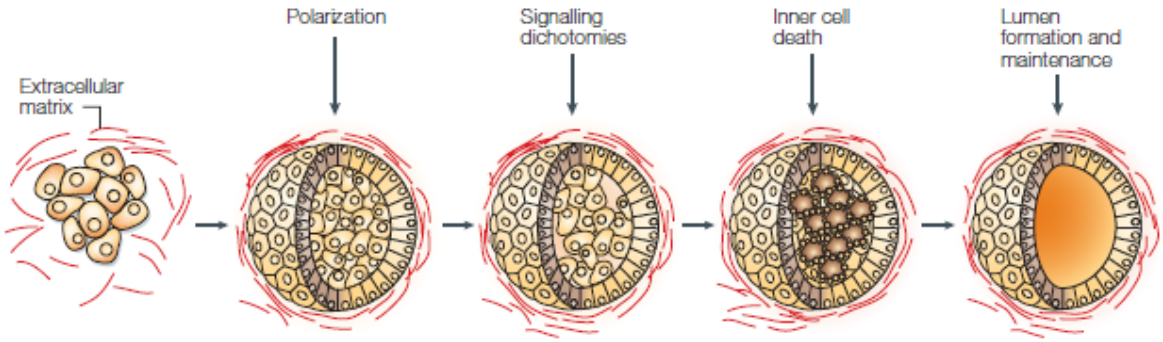

Figure 31: Formation of cysts. Formation cyst starts from a single cell, which proliferate and form a spherical. Then cells inside the spherical go into apoptosis resulting in a cyst with a lumen. The inner membrane represents the apical side and the outer membrane the baso-lateral side. (From Debnath, 2005)

Figure 32 shows a MDCK cyst stained against DNA, actin and ZO-1. The nuclei are forming a nice ring and the tight junction protein ZO-1, which is localised at the apical junctional complex, shows that the apical membrane faces towards the inside lumen.

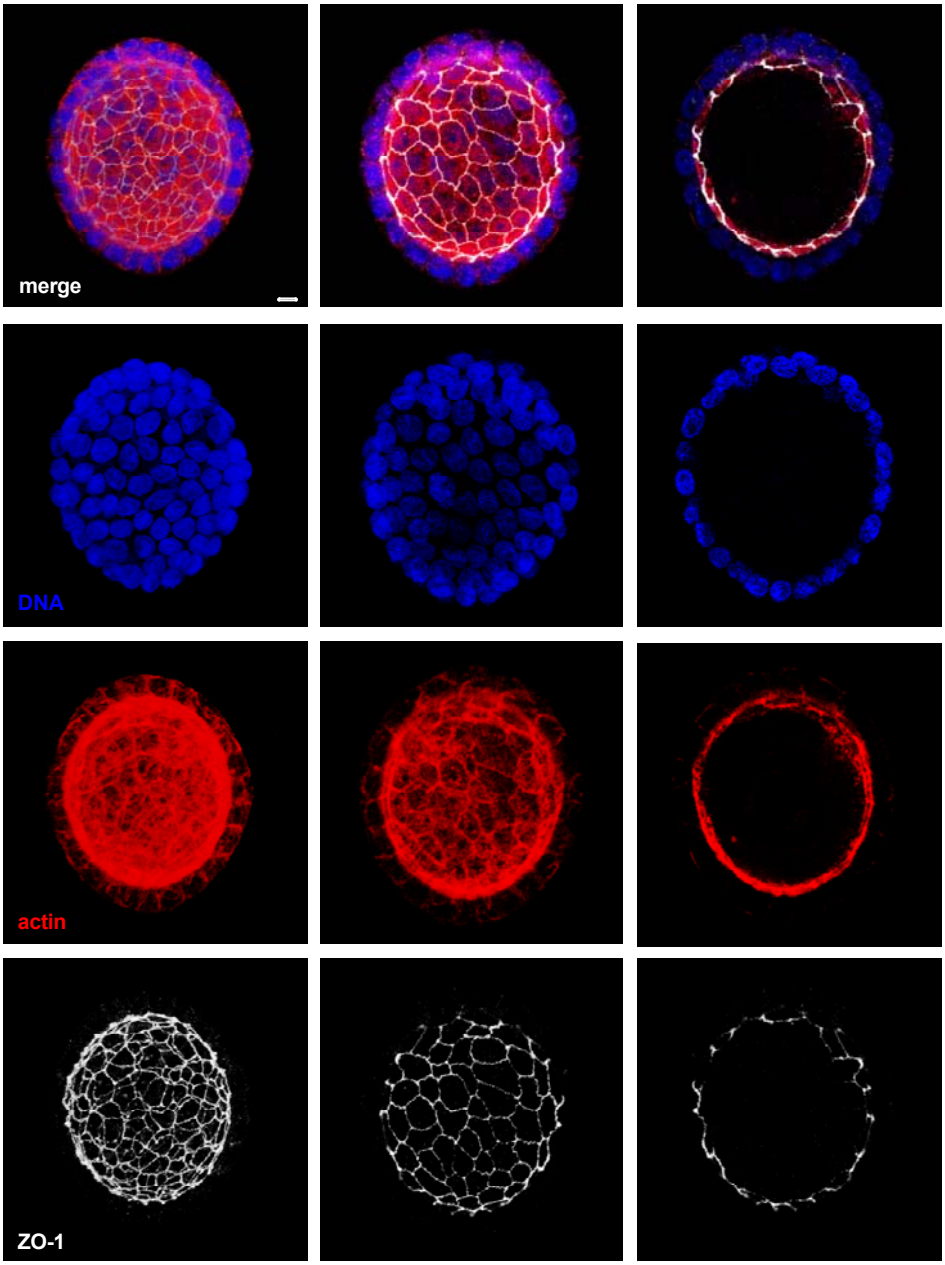

Figure 32: MDCK cyst: Confocal microscopy images of MDCK cysts. 3-D reconstructions of confocal z-stacks. DNA (blue), actin (red) and ZO-1 (white). Bar 10µm.

3.3.6.1 Infection of MDCK cyst

MDCK cysts were infected with *H. pylori* wt and two *H. pylori* mutants. The *H. pylori* EPISA mutant has mutated EPIYA A and B motifs and deleted EPIYA C motifs (Figure 9) and the *H. pylori* ΔCagA mutant can adhere to MDCK cells but cannot inject the CagA through the Type IV secretion system. Figure 33A shows *H. pylori* adhering to an AGS cell. Figure 33B shows *H. pylori* adhering to MDCK cysts.

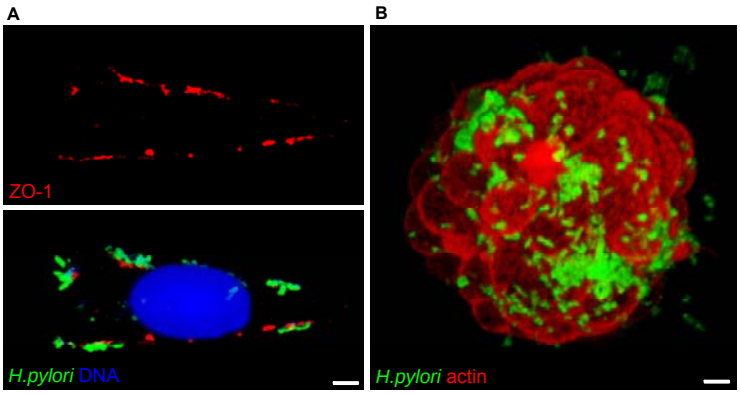

Figure 33: *H. pylori* adheres to AGS cells or MDCK cysts. A) AGS cells infected with H. pylori (green) H. pylori is found at the tight junction protein ZO-1(red). DNA (blue). Bar 1µm B) H. pylori adheres to MDCK cysts. 3-D reconstructions of confocal z-stacks Actin (red). Bar 10µm.

Infected cysts lost their apical-basolateral orientation, started to multilayer and lost their spherical structure (Figure 34B and B‘). This was independent of CagA phosphorylation or CagA translocation since *H. pylori* EPISA and ΔCagA mutants also induced a loss of apical-basolateral orientation (Figure 34C and D).

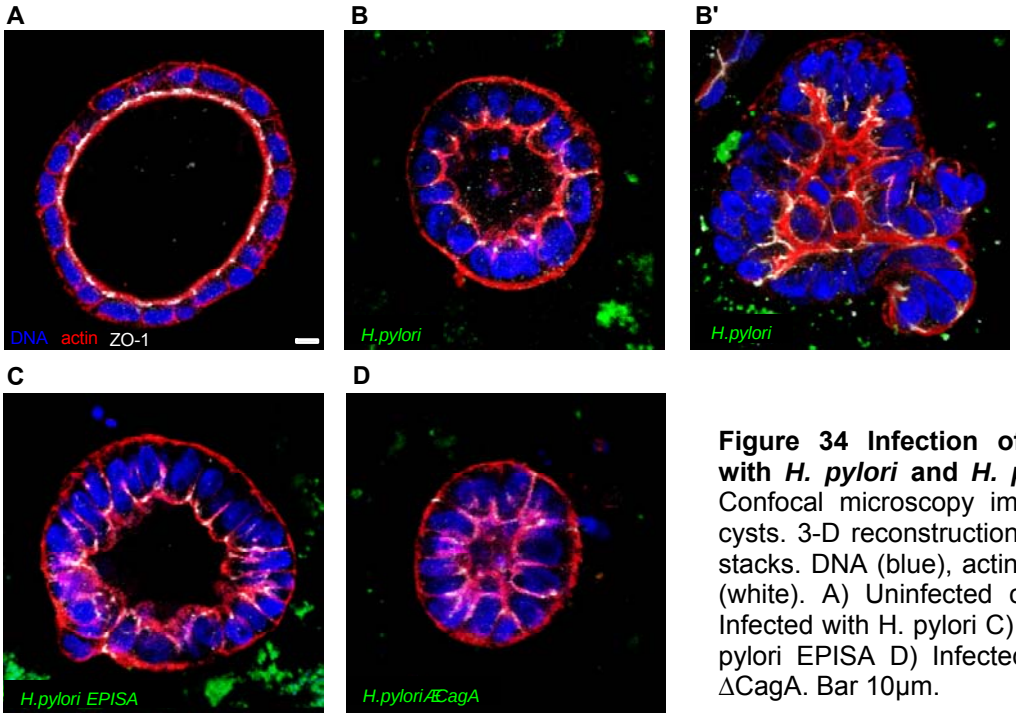

Figure 34 Infection of MDCK cysts with *H. pylori* and *H. pylori* mutants. Confocal microscopy images of MDCK cysts. 3-D reconstructions of confocal z-stacks. DNA (blue), actin (red) and ZO-1 (white). A) Uninfected cyst. B and B‘) Infected with H. pylori C) Infected with H. pylori EPISA D) Infected with H. pylori ΔCagA. Bar 10µm.

Infection of the MDCK cysts with H. pylori is not a suitable model to study effects of CagA, since the infection, independently of CagA, leads to the destruction of cysts.

3.3.6.2 MDCK cysts expressing CagA and CagA mutants

MDCK cells stable and inducible expressing CagA and mutant CagA were used for 3D culture. When cysts were developed, CagA expression was induced. After 48 hours cysts were fixed and stained.

After induction of CagA expression cysts lost their apical orientation, started to proliferate and were destroyed. This was restricted to the C-terminus of CagA since a CagA mutant expressing CagA 800-1216 resulted in destroyed cysts whereas expression of the N-terminal part of CagA (CagA 1-800) containing the MBD did not have any effects on the MDCK cysts.

The MBD had no influence on the destruction of cysts nor can it abolish the effect of the C-terminus of CagA, since expression of the CagA mutants CagA 200-1216 lacking the MBD as well as the mutant CagA Δ200-800, which targets CagA C-terminus to a different membrane structure, also resulted in the destruction of the cysts.

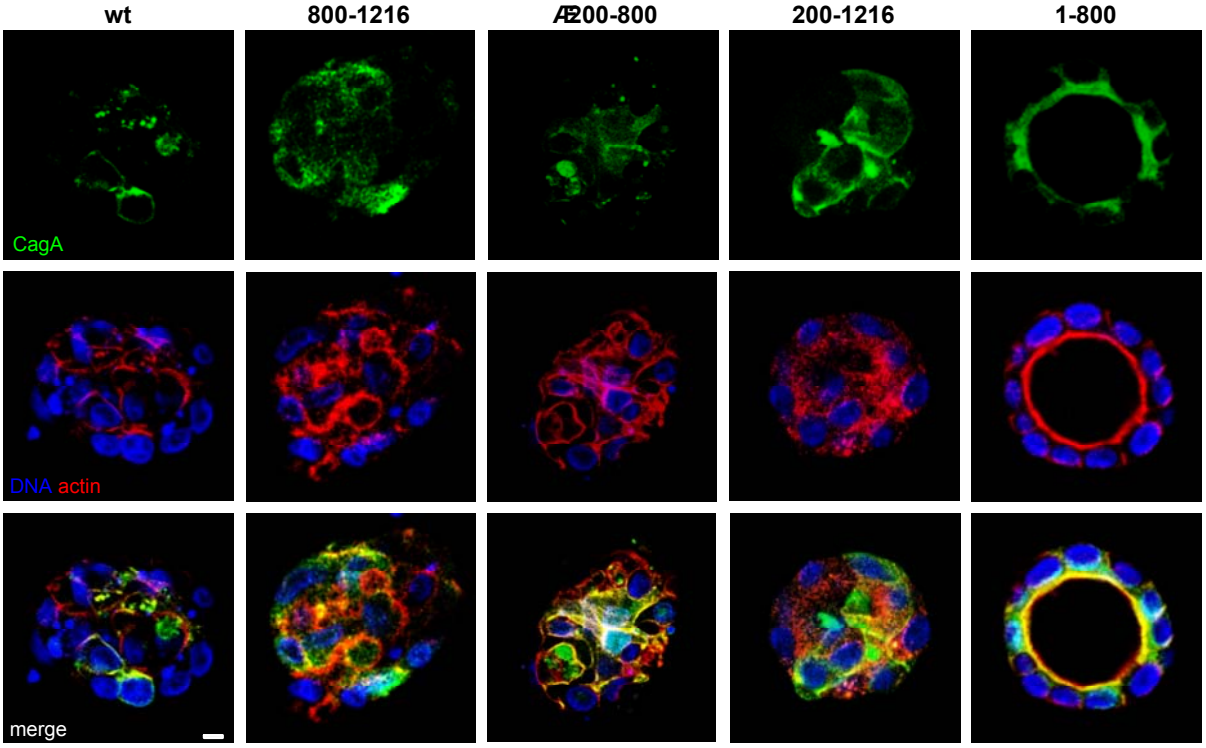

Figure 35: CagA and mutant CagA expressed in MDCK cysts. Confocal microscopy images: 3-D reconstructions of confocal z-stacks. MDCK cysts expressing CagAwt, 800-1216, Δ200-800, 200-1216, 1-800 (green) stained against DNA (blue) ZO-1 (red). Bar 10µm

Subsequently the question arose as to what the mechanisms are for the disruption of the CagA C-terminus expressing cysts.

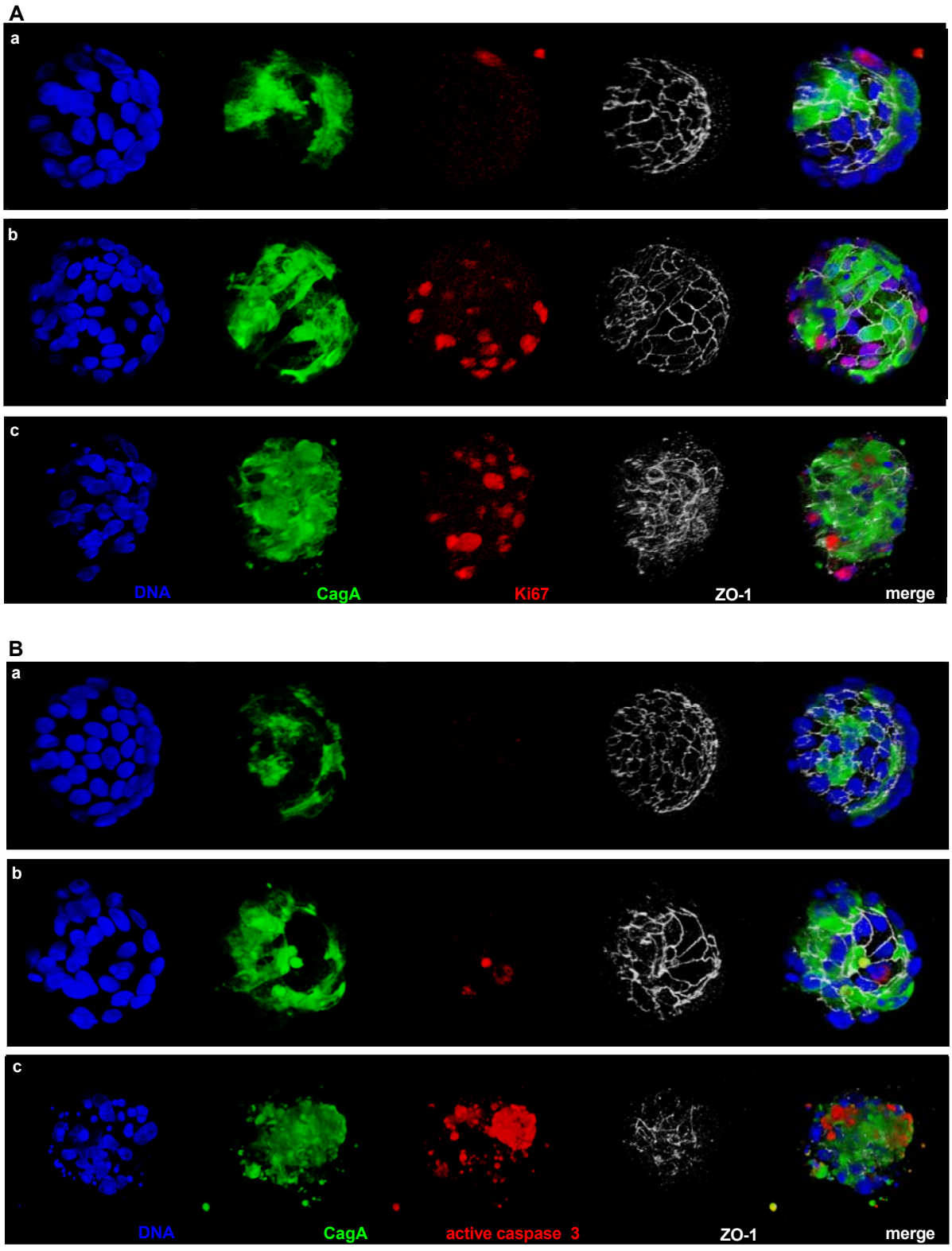

Figure 36: Proliferation and Apoptosis of CagA expressing MDCK cysts. MDCK cysts expressing CagAΔ200-800 (green) stained against DNA (blue) ZO-1 (white) and A) Ki67 (red) B) active Caspase3. In (a) cysts are shown which express CagA but still posses the cystic appearance. In (b) cysts are shown which multilayer and in (c) cysts already were apoptotic with disrupted cell structures. Bar 10µm.

Cysts were stained with an antibody against Ki67, a marker for proliferation and with an antibody against active Caspase 3, which is a marker for apoptosis. After induction of CagA expression, cells started to proliferate and to multilayer. Simultaneously Caspase 3 was activated and cells underwent apoptosis resulting in a total destruction of the cysts.

After establishing that CagA induced proliferation and subsequent induction of apoptosis of MDCK cysts, which was restricted to the C-terminus of CagA, it was investigated whether the CM/CRIPYA motif is involved in these processes. When CagAΔPar1 and CagA800-1216ΔPar1 were expressed in MDCK cysts, they did keep their spherical shape and did not proliferate or go into apoptosis. This was independent of membrane localisation, as CagAΔPar1 was located to the membrane whereas CagA800-1216ΔPar1 was located to the cytoplasm (Figure 37). These results show an involvement of the CM/CRIPYA motif in the proliferation and disorganisation of cysts, which is followed by apoptosis and total destruction.

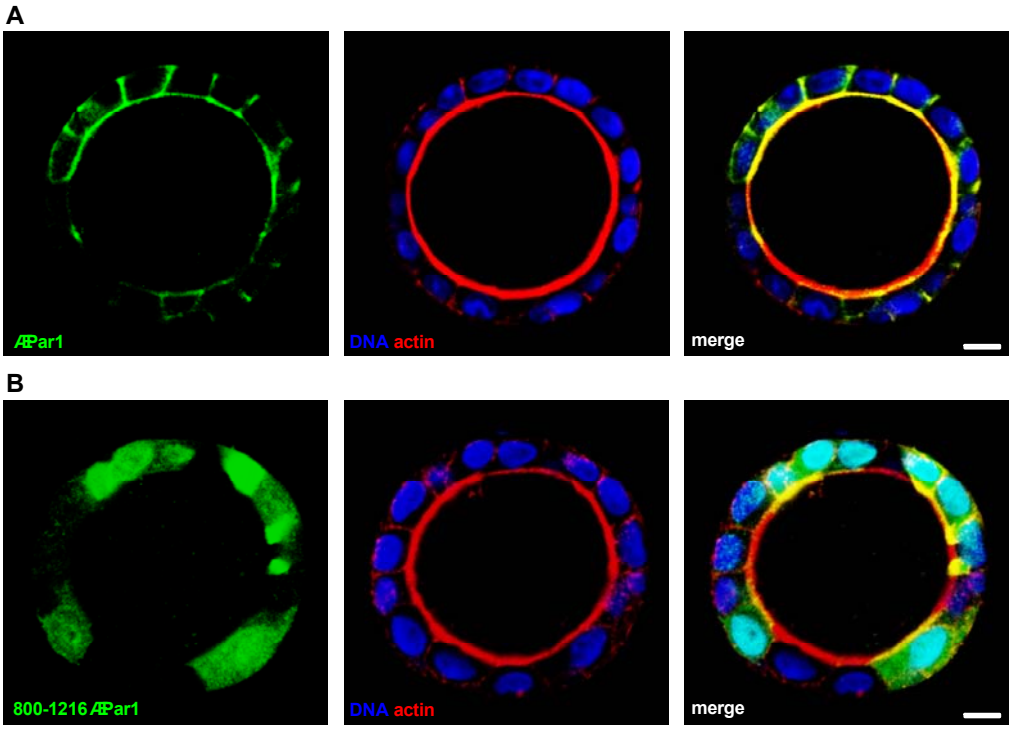

Figure 37: CagAΔPar1 and CagA800-1216ΔPar1 were expressed in MDCK cysts. Confocal microscopy images: 3-D reconstructions of confocal z-stacks. MDCK cysts expressing A) CagAΔPar1 or B) CagA800-1216ΔPar1(green) stained against DNA (blue) actin (red). Bar 10µm

4 Discussion

H. pylori CagA protein is a high risk factor for developing gastric cancer. *In vitro*, the known biological effects are assigned to the C-terminus of CagA. Little is known about the role of the remaining two-thirds of this 130 kDa protein in host cells. The present work addressed the question of what functions can be assigned to the N-terminus of CagA and how it affects host cell responses.

Upon delivery into the host gastric epithelial cells, CagA physically and functionally interacts with a number of target molecules in phosphorylation dependent and independent manners. These interactions may contribute to the malignant transformation of mammalian cells. Nonetheless, the exact role of CagA in tumour genesis still remains obscure. The presented work aids clarification of the published data, which at first glance appeared to be contradictory. Additionally, there are many natural variances in the CagA gene leading to different experimental results. Also the differences in the specific amino acid codes between Eastern and Western CagA in addition to the number of EPIYA and CM/CRPIA motifs is critical.

In vitro CagA expression induces two opposing phenotypes. The migratory phenotype where polarised cells constrict the apical surface and become invasive (Bagnoli et al., 2005) and the multi-layering phenotype with extrusion of cells towards the apical membrane, which is mediated by interaction of the CM/CRPIA with Par1b, a protein at the lateral membrane (Böhm et al., 1997; Saadat et al., 2007). This work provides data, showing that subcellular membrane localisation can influence the appearance of these phenotypes.

4.1 Localisation of CagA

This work could identify a membrane-binding domain in the N-terminal part of CagA (AA 1-200) and additionally a second part of CagA (AA 200-1216), which independently of the MBD localises to the plasma membrane albeit to different membrane compartments. These results help to clarify published data that appeared to be inconsistent with each other. One report described that EPIYA motifs mediate membrane attachment of CagA, whereas another report demonstrated that the N-terminus of CagA directs the protein to the plasma membrane of epithelial cells independent of EPIYA motifs (Higashi et al., 2005; Bagnoli et al., 2005). The presented data shows that CagA N-terminus indeed has a domain, which localises it to the membrane namely CagA 1-200, which is defined the CagA MBD here. It also

shows that the CagA C-terminus (AA 800-1216) localises to the cytoplasm when evaluated by immunofluorescence consistent with the observation made by Bagnoli et al. (Bagnoli et al., 2005). However a membrane-pelleting assay revealed that membrane interaction is masked by the immunofluorescence signal in the cytoplasm and that CagA 800-1216 in fact interacts with the membrane compartment, but considerably less compared to CagA 200-1216. CagA 200-1216 was found to strongly interact with the membrane when assed in the biochemical membrane-pelleting assay. It consists of two parts CagA 200-800 and 800-1216, which interact with each other in trans and subsequently localise to the membrane. When expressed by itself, both parts are localised partly in the cytoplasm and partly at the membrane.

The MBD targets a different subcellular membrane structure than the C-terminal part of CagA (200-1216). The CagA 1-200 MBD localises to cell-cell contacts at newly formed lateral membranes in non-polarized epithelia and is distributed along the lateral and apical membrane in polarized epithelial cells, whereas CagA 200-1216 is evenly distributed along the membrane in non-polarized epithelial cells and in polarized cells primarily focused to the apical membrane.

This raises the question why CagA has a MBD in the N-terminus in addition to it's ability to localise to the membrane via the amino acids 200-1216 and how it affects host cell responses. A variety of functional assays were performed to address this question and revealed an inhibiting effect of the CagA MBD on host cell responses induced by CagA 200-1216.

Data presented in this study suggest that subcellular localisation of CagA regulates it's function.

4.2 Functional Assays reveal the function of CagA MBD

The interaction of phosphorylated CagA with SHP-2 leads to activation of SHP-2 phosphatase resulting in an elongated cell shape (Higashi et al., 2002b; Higashi et al., 2005). The present study shows that targeting CagA 800-1216 to a different membrane compartment via the N-terminal MBD decreases cell elongation significantly. The CagA 1-200 MBD, which has no effect on these host responses by itself, inhibits cell elongation induced by signalling motifs in the C-terminus of CagA. This is a very strong effect since deleting the MBD from CagA wt resulted in a comparable level of elongation of CagA 200-1216 and CagA 800-1216 respectively. These data suggest that CagA 200-1216 is targeted to a different cellular

substructure via the CagA MBD resulting in reduced SHP-2 interaction and hence reduced formation of protrusions, which is a characteristic of the migratory phenotype.

The idea that CagA subcellular localisation regulates CagA function is emphasized by the observation made in regard to CagA induced apical constriction. The C-terminal part of CagA (200-1216), which is targeted to the apical membrane elicits a significantly stronger apical constriction response than CagA wt. The CagA 1-200 MBD inhibits CagA 200-1216 induced apical constriction. The constriction of apical surface is part of the migratory phenotype in CagA expressing cells, where cells move underneath neighbouring cells (Bagnoli et al., 2005). This is opposite to the multi-layering phenotype, where cells become extruded towards the apical membrane (Saadat et al., 2007). The inhibitory effect of CagA 1-200 on the migratory phenotype would allow CagA to exert its oppositional phenotypic response on polarized epithelia.

CagA destabilizes the E-cadherin/β-catenin complex at cell-cell junctions, which causes loss of cell-cell adhesion and an increase of cytoplasmic β-catenin resulting in TCF/β-catenin transcriptional activation (Franco et al., 2005; Murata-Kamiya et al., 2007; Suzuki et al., 2005). This effect only manifests when TCF/Lef signalling is constitutively active. Since MDCK cells don't have constitutively active TCF-Lef signalling, CagA didn't increase cytoplasmic b-Catenin. Therefore, effects of the CagA 1-200 MBD on β-catenin transcriptional activity were tested in a gastric epithelial cell line NCI-N87, which forms adherens junctions and has constitutive TCF/β-catenin transcriptional activity (Caca et al., 1999). CagA behaves similarly in these cells as shown for MDCK cells (data not shown). Transient expression of CagA wt increased the amount of cytoplasmic b- Catenin significantly. Deleting the CagA MBD form CagA wt further increased TCF/β-catenin transcriptional activity. As assessed by immunofluorescence CagA MBD co-localises with β-catenin at the lateral membrane, suggesting a role in stabilising the cadherin/catenin complex. This result is another example of the concept that CagA function can be regulated by the interplay of the MBD with membrane substructures.

An unexpected finding of this work was that the MBD of CagA enhances the formation of cell-cell adhesion considerably. It counteracts the effect of the CagA 200-1216, which decreases the rate of formation of cell-cell contacts and weakens their strength significantly. CagA wt expressing cells were not different in the rate of

cell-cell contact formation or in the strength of formed contacts compared to control cells, showing that the MBD neutralises the effect of the CagA C-terminus (200-1216). This observation is contrary to the well-established fact that CagA induces loss of cell-cell adhesion in sub-confluent cells mediated by phosphorylation dependent and independent host signalling via the EPIYA and CM/CRPIA motifs (Churin et al., 2003; Hatakeyama, 2008; Higashi et al., 2002a; Suzuki et al., 2009). This discrepancy could be due to the lack of cell-extracellular matrix (ECM) interaction in the cell-cell adhesion assay used in this study. Cell-cell and cell-ECM adhesion are interdependent processes (Etienne-Manneville, 2008; Imamichi and Menke, 2007).

Taken together the functional data suggest that the MBD localises CagA wt to basolateral membrane substructures and regulates divers functions of CagA by probably stabilizing the cadherin/catenin protein complex.

4.3 Role of the EPIYA and CM/CRIPYA motif on host cell responses independent of the MBD

In 4.2 it was shown that CagA MBD influences host cell responses by targeting it to different substructures and stabilising the cadherin/catenin complex. However several other functional assays revealed a limited influence of the MBD on effects triggered by the CM/CRIPYA motif. One example is the barrier function of polarised epithelial cells, which is disrupted in CagA expressing cells (Amieva et al., 2003; Lu et al. 2008). In contrast to published data showing that CagA decreases TER in already polarised monolayers the present experimental setup followed the formation of the barrier function of polarising epithelial cells, hence tight junction formation by measuring the flux of ions via TER. These experiments revealed that the formation of the barrier function is delayed in CagA expressing cells. This effect was restricted to signalling motifs in the CagA C-terminus. Targeting CagA to different substructures via the MBD did not potentiate or reverse barrier formation defects induced by CagA. Consistent with this observation is that the MBD by itself did not have any effect on barrier formation; it could not elevate nor attenuate the tight junction formation.

Published data state that CagA induced disruption of the barrier function is reversible by co-expression of Par1b, a protein that interacts with CagA through the CM/CRIPYA motif (Saadat et al., 2007). A CagA mutant, which has the CM/CRIPYA motifs deleted had a normal development of the barrier function. This shows that the

barrier formation defect of CagA expressing cells is dependent on the CM/CRIPYA motif, which is consistent with published data (Lu et al., 2008).

Another example of the limited influence of the MBD on effects triggered by the CM/CRIPYA motif is the expression of CagA in 3D tissue culture. CagA expressing cysts lost their apical-basolateral orientation, started to proliferate and multilayer, which was followed by the induction of apoptosis resulting in total destruction of the cysts. Again this process was restricted to the C-terminal CM/CRIPYA signalling motif, since a deletion mutant that has the CM/CRIPYA motifs deleted resulted in healthy cysts.

Having witnessed such a strong influence of the CM/CRPIYA motif on host signalling it was an obvious step to also study CM/CRPIYA deletion mutants in the elongation assay. Older reports state that the phosphorylation of the EPIYA motif is essential for the elongation phenotype (Bagnoli et al., 2005; Stein et al., 2002). But recent data shows that the CM/CRPIA motif causes cell elongation in a phosphorylation-independent manner (Suzuki et al., 2009).

The present data helps to clarify this discrepancy and shows again a strong effect of the CM/CRIPYA motif signalling. The formation of protrusion was almost completely abolished in a CagA 800-1216 ΔPar1 deletion mutant, which has a deletion from the first to the last of the three CM/CRPIA motifs. In contrast, expression of a CagA 800-1216 EPISA C mutant, which has the tyrosine residues in EPIYA C motifs mutated to serine resulted in a reduced formation of protrusions showing that the deletion of EPIYA C motifs in the CagA 800-1216 ΔPar1 mutant did not abolish the protrusions. Moreover a CagA 800-1216$_{EPISA}$ mutant that cannot be phosphorylated, because it has the tyrosine residues mutated to serine in the EPIYA motifs A and B and the EPIYA C region deleted, but still contains one CM/CRPIA, can still elongate polarized epithelial cells. This is in line with published data stating that the CM/CRPIA motif causes cell elongation in a phosphorylation-independent manner (Suzuki et al., 2009).

Interestingly, there is data in the literature stating that a full-length CagA protein (CagA FL$_{EPISA}$) with the same mutation as CagA 800-1216$_{EPISA}$ could not elongate cells (Bagnoli et al., 2005; Stein et al., 2002). The data was interpreted to state that the EPIYA motif and hence phosphorylation of CagA is necessary for cell elongation and the migratory phenotype. Regarding the data presented in this study, it is implicit that effects observed by deleting larger segments of the C-terminus of CagA as seen

with CagA FL_{EPISA} maybe due to a weakening of membrane attachment rather than due to lack of the signalling motif. The effect of the remaining CM/CRPIA motif in CagA FL_{EPISA} on cell elongation could be neutralized, because the deletion weakens membrane binding via the C-terminus in CagA FL_{EPISA} and therefore it is targeted to a different subcellular membrane structure via the CagA 1-200 MBD. This is another strong hint that subcellular localisation mediated by the CagA MBD is a regulator of CagA functions in host cells.

Interestingly, the constriction of the apical surface in CagA expressing cells is dependent on the EPIYA C motifs since a mutant that has the tyrosin residues in the EPIYA C motifs mutated to serine didn't constrict the apical surface. This data suggests that the constriction phenotype is independent of the CM/CRPIA signalling motif.

4.4 Natural variances in the CagA gene lead to different experimental results

It has been shown so far, that much of the inconsistency in the data presented in the literature can be traced back to experimental procedures or false interpretation of data.

Another major factor for inconsistency in published data has not been discussed yet. There are many natural variances in the CagA gene, such as the differences in amino acid codes between Eastern and Western CagA as well as the number of EPIYA and CM/CRPIA motifs, leading to different experimental results. For example it was shown that Eastern CagA is more potent in inducing host cell responses than Western CagA (Lu et. al, 2008).

Differences in amino acid codes may lead to an attenuated pathogenicity of Western CagA (Figure 38). When CagA 1-200 from an Eastern CagA strain was expressed in MDCK cells, the immune fluorescent signals gave the impression that Eastern CagA 1-200 has less membrane binding capacity then Western CagA (Data not shown). Also in a membrane-pelleting assay the amount of membrane bound Eastern CagA seemed to be less than that of Western CagA (Data not shown). A reduced membrane binding capacity could be an explanation for the lower pathogenicity of Western CagA strains.

Interestingly, when CagA MBD in CagA wt is replaced by CagA 1-200 from an Eastern *H. pylori* strain, the formation of protrusions is reduced. From the data presented earlier, one would expect an elevated formation of protrusions. Unfortunately it was not possible within this work to elucidate the effects of Eastern

CagA in a more detailed fashion. But these data clearly show that variances in the CagA gene lead to different experimental results.

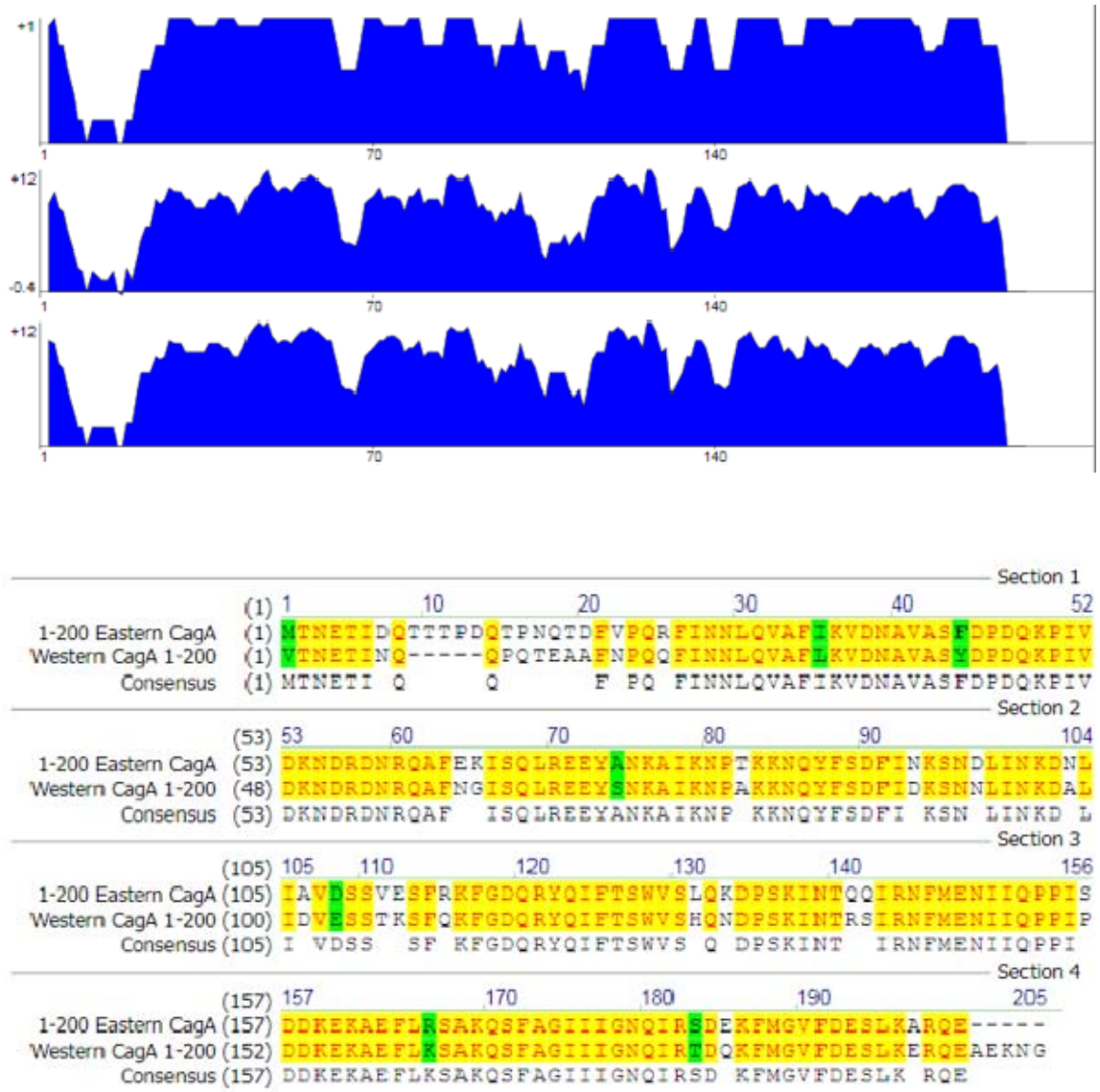

Figure 38: Sequence alignment of a Western and Eastern CagA strain.

4.5 Conclusion and Outlook

The presented data shows that CagA function can be regulated by its subcellular localisation. Natural variances in the CagA gene may lead to altered pathogenicity of different CagA strains. Especially dissimilar binding capacity of CagA MBD in Eastern and Western strains could explain the higher prevalence for development of gastric cancer in patients infected with an East Asian CagA positive *H. pylori* strain.

Although this study did not test the role of CagA for carcinogenesis, the data implies that incidences which weaken the interaction of the CagA 1-200 MBD with cell-cell junctions, could lead to an increase in TCF/β-catenin transcriptional activity and could be important for gastric carcinogenesis, since increased TCF/β-catenin transcriptional activity is associated with cancer formation (Clevers, 2006).

Identifying potential binding partners of CagA mutants would have been complementary to the functional data received in this work. Unfortunately identifying proteins, which are part of the cell membrane, is a complicated task. A standard method for identification of binding partners would be immune precipitation. Here immune precipitation was not a useful tool to identify direct binding partners of CagA and CagA mutants, since membrane proteins are part of big protein complexes and CagA co-immunoprecipitates with these complexes. During this work it was not possible to apply complex methods to address the question of potential binding partners. But CagA mutants created in this work are a useful tool for future studies and could help to identify new binding partners and elucidate the signalling pathways involved in the functional regulation of CagA induced host cell effects.

Earlier the question was asked why CagA has an additional MBD when the CagA C-terminus independently of the MBD localises to the membrane. One possible explanation may be the interaction with proteins, which are confined to the specific membrane substructures. CagA is injected at the apical membrane were it initially can be found (Wessler and Backert, 2008; Amieva et al., 2003). But many proteins that CagA interferes with are confined to basal-lateral membranes in polarised epithelia. (Böhm et al., 1997; Nelson et al., 1990; Stewart et al., 2002; Vogelmann and Nelson, 2005). CagA may be between two oppositional forces. The CagA 200-1216 has a strong binding capacity to the apical membrane where it constricts it leading to the migratory phenotype, whereas CagA MBD distributes along the lateral membrane. CagA MBD is counteracting the strong apical localisation of CagA 200-1216, which may be essential for the interaction of CagA with other proteins in the host cell that are localized at basal-lateral membranes. Functional assays revealed that CagA 1-200 could attenuate effects of CagA 200-1216 by localising it to different cellular substructures. In conclusion this work provides a useful insight into the dependency of membrane localisation of CagA in regards to altered host cell function.

5 Abstract

The infection with a CagA positive *H. pylori* is associated with an increased risk for developing gastric cancer. The *H. pylori* protein CagA is the only know protein, which is delivered into the host cells of the gastric mucosa via a Type IV secretion system. After injection, CagA localises to the membrane of the epithelial cells resulting in a variety of host cell responses. Much of the ongoing research focuses on the C-terminal part of CagA with its EPIYA and CM/CRPIA motif. Less effort has been made on the N-terminal part of CagA. This work elucidates the role of the CagA N-terminus, by focusing on the CagA protein as a single factor in an *in vitro* tissue culture model.

A novel membrane-binding domain (MBD) of CagA was identified and its role on host cell responses was investigated in a variety of functional assays. The data presented in this work demonstrates that the MBD of CagA can influence host cell signalling by targeting CagA to different membrane substructures. It is shown that the MBD of CagA inhibits the migratory phenotype, which is induced by the CagA C-terminus and is characterised by cell elongation and constriction of the apical surface. The MBD also increases cell-cell adhesion and inhibits TCF/b-catenin transcriptional activity mediated by the C-terminus of CagA. Additionally a second part of CagA containing the EPIYA and CM/CRPIA motif was identified which binds to membrane structures in polarized epithelial cells independently of the membrane-binding domain. Several functional assays revealed that many effects, which are caused by the CM/CRPIA motif, are independent of sub-cellular localisation of CagA, showing a limited influence of the CagA MBD.

Nonetheless, the presented work is a significant contribution to clarify the role of the CagA N-terminus on host cell responses and establishes a new concept that targeting CagA to different membrane substructures determines CagA cell signalling. It implicates that differences in host factors or variations of the CagA gene would alter the localisation of CagA to membrane structures and in conclusion modify host cell responses involved in carcinogenesis.

6 References

Amieva, M. R., Vogelmann, R., Covacci, A., Tompkins, L. S., Nelson, W. J., and Falkow, S. (2003). Disruption of the epithelial apical-junctional complex by Helicobacter pylori CagA. Science *300*, 1430-1434.

Asahi, M., Azuma, T., Ito, S., Ito, Y., Suto, H., Nagai, Y., Tsubokawa, M., Tohyama, Y., Maeda, S., Omata, M., *et al.* (2000). Helicobacter pylori CagA protein can be tyrosine phosphorylated in gastric epithelial cells. J Exp Med *191*, 593-602.

Backert S., Müller E.C., Jungblut P.R. and Meyer T.F. (2001). Tyrosine phosphorylation patterns and size modification of the Helicobacter pylori CagA protein after translocation into gastric epithelial cells. Proteomics 1, pp. 608-17

Bagnoli, F., Buti, L., Tompkins, L., Covacci, A., and Amieva, M. R. (2005). Helicobacter pylori CagA induces a transition from polarized to invasive phenotypes in MDCK cells. Proc Natl Acad Sci U S A *102*, 16339-16344.

Barth, A. I., Pollack, A. L., Altschuler, Y., Mostov, K. E., and Nelson, W. J. (1997). NH2-terminal deletion of beta-catenin results in stable colocalization of mutant beta-catenin with adenomatous polyposis coli protein and altered MDCK cell adhesion. The Journal of cell biology *136*, 693-706.

Blaser, M. J., Perez-Perez, G. I., Kleanthous, H., Cover, T. L., Peek, R. M., Chyou, P. H., Stemmermann, G. N., and Nomura, A. (1995). Infection with Helicobacter pylori strains possessing cagA is associated with an increased risk of developing adenocarcinoma of the stomach. Cancer research *55*, 2111-2115.

Böhm, H., Brinkmann, V., Drab, M., Henske, A., and Kurzchalia, T. V. (1997). Mammalian homologues of C. elegans PAR-1 are asymmetrically localized in epithelial cells and may influence their polarity. Current biology: CB *7*, 603-606.

Brandt, S., Kwok, T., Hartig, R., Konig, W., and Backert, S. (2005). NF-kappaB activation and potentiation of proinflammatory responses by the Helicobacter pylori CagA protein. Proc Natl Acad Sci USA *102*, 9300-9305.

Brenner, H., Arndt, V., Stegmaier, C., Ziegler, H., and Rothenbacher, D. (2004). Is Helicobacter pylori infection a necessary condition for noncardia gastric cancer? Am J Epidemiol *159*, 252-258.

Caca, K., Kolligs, F. T., Ji, X., Hayes, M., Qian, J., Yahanda, A., Rimm, D. L., Costa, J., and Fearon, E. R. (1999). Beta- and gamma-catenin mutations, but not E-cadherin inactivation, underlie T-cell factor/lymphoid enhancer factor transcriptional deregulation in gastric and pancreatic cancer. Cell Growth Differ *10*, 369-376.

Campbell, R. E., Tour, O., Palmer, A. E., Steinbach, P. A., Baird, G. S., Zacharias, D. A., and Tsien, R. Y. (2002). A monomeric red fluorescent protein. Proc Natl Acad Sci USA *99*, 7877-7882.

Churin, Y., Al-Ghoul, L., Kepp, O., Meyer, T. F., Birchmeier, W., and Naumann, M. (2003). Helicobacter pylori CagA protein targets the c-Met receptor and enhances the motogenic response. J Cell Biol *161*, 249-255.

Clevers, H. (2006). Wnt/beta-catenin signaling in development and disease. Cell *127*, 469-480.

Debnath J. and Brugge, J.S., (2005). Modelling glandular epithelial cancers in three-dimensional cultures. Nat Rev Cancer 5, 675-88.

Ehrlich, J. S., Hansen, M. D., and Nelson, W. J. (2002). Spatio-temporal regulation of Rac1 localization and lamellipodia dynamics during epithelial cell-cell adhesion. Dev Cell *3*, 259-270.

Ernst, P. B., and Gold, B. D. (2000). The disease spectrum of Helicobacter pylori: the immunopathogenesis of gastroduodenal ulcer and gastric cancer. Annu Rev Microbiol *54*, 615-

Etienne-Manneville, S. (2008). Polarity proteins in migration and invasion. Oncogene *27*, 6970-6980.

Franco, A. T., Israel, D. A., Washington, M. K., Krishna, U., Fox, J. G., Rogers, A. B., Neish, A. S., Collier-Hyams, L., Perez-Perez, G. I., Hatakeyama, M.*, et al.* (2005). Activation of beta-catenin by carcinogenic Helicobacter pylori. Proc Natl Acad Sci USA *102*, 10646-10651.

Hatakeyama, M. (2008). SagA of CagA in Helicobacter pylori pathogenesis. Curr Opin Microbiol *11*, 30-37.

Higashi, H., Tsutsumi, R., Fujita, A., Yamazaki, S., Asaka, M., Azuma, T., and Hatakeyama, M. (2002a). Biological activity of the Helicobacter pylori virulence

factor CagA is determined by variation in the tyrosine phosphorylation sites. Proc Natl Acad Sci USA *99*, 14428-14433.

Higashi, H., Tsutsumi, R., Muto, S., Sugiyama, T., Azuma, T., Asaka, M., and Hatakeyama, M. (2002b). SHP-2 tyrosine phosphatase as an intracellular target of Helicobacter pylori CagA protein. Science *295*, 683-686.

Higashi, H., Nakaya, A., Tsutsumi, R., Yokoyama, K., Fujii, Y., Ishikawa, S., Higuchi, M., Takahashi, A., Kurashima, Y., Teishikata, Y., Tanaka, S., Azuma, T. and Hatakeyama, M., (2004). Helicobacter pylori CagA induces Ras-independent morphogenetic response through SHP-2 recruitment and activation. J. Biol. Chem. 279 pp. 17205-16

Higashi, H., Yokoyama, K., Fujii, Y., Ren, S., Yuasa, H., Saadat, I., Murata-Kamiya, N., Azuma, T., and Hatakeyama, M. (2005). EPIYA motif is a membrane-targeting signal of Helicobacter pylori virulence factor CagA in mammalian cells. J Biol Chem *280*, 23130-23137.

Huber, M.A., Kraut, N. and Beug, H., (2005). Molecular requirements for epithelial-mesenchymal transition during tumor progression. Curr. Opin. Cell Biol. 17, 548-558

Imamichi, Y., and Menke, A. (2007). Signaling pathways involved in collagen-induced disruption of the E-cadherin complex during epithelial-mesenchymal transition. Cells, tissues, organs *185*, 180-190.

Ishikawa S., Ohta T. and Hatakeyama M. (2009). Stability of Helicobacter pylori CagA oncoprotein in human gastric epithelial cells. FEBS LETTERS 583 (14) pp. 2414-8

Kuipers, E. J., Thijs, J. C., and Festen, H. P. (1995). The prevalence of Helicobacter pylori in peptic ulcer disease. Aliment Pharmacol Ther *9 Suppl 2*, 59-69.

Kurashima, Y., Murata-Kamiya, Kikuchi, K., N., Higashi, H., Azuma, T., Kondo, S. and Hatakeyama, M. (2008). Deregulation of beta-catenin signal by Helicobacter pylori CagA requires the CagA-multimerization sequence. Int J Cancer 122 pp. 823-31.

Lu, H. S., Saito, Y., Umeda, M., Murata-Kamiya, N., Zhang, H. M., Higashi, H., and Hatakeyama, M. (2008). Structural and functional diversity in the

PAR1b/MARK2-binding region of Helicobacter pylori CagA. Cancer Sci *99*, 2004-2011.

Malfertheiner, P., Sipponen, P., Naumann, M., Moayyedi, P., Megraud, F., Xiao, S. D., Sugano, K., and Nyren, O. (2005). Helicobacter pylori Eradication Has the Potential to Prevent Gastric Cancer: A State-of-the-Art Critique. Am J Gastroenterol *100*, 2100-2115.

Marshall, B. J., and Warren, J. R. (1984). Unidentified curved bacilli in the stomach of patients with gastritis and peptic ulceration. Lancet *1*, 1311-1315.

Mohi, M. G., and Neel, B. G. (2007). The role of Shp2 (PTPN11) in cancer. Curr Opin Genet Dev *17*, 23-30.

Murata-Kamiya, N., Kurashima, Y., Teishikata, Y., Yamahashi, Y., Saito, Y., Higashi, H., Aburatani, H., Akiyama, T., Peek, R., Azuma, T., and Hatakeyama, M. (2007). Helicobacter pylori CagA interacts with E-cadherin and deregulates the beta-catenin signal that promotes intestinal transdifferentiation in gastric epithelial cells. Oncogene *26*, 4617-26.

Muthuswamy, S. K., Li, D., Lelievre, D., Bissell, M. J. and Brugge. J. S., (2001). ErbB2, but not ErbB1, reinitiates proliferation and induces luminal repopulation in epithelial acini. Nature Cell Biology 3, 785-92

Naito, M., Yamazaki, T., Tsutsumi, R., Higashi, H., Onoe, K., Yamazaki, S., Azuma, T., and Hatakeyama, M. (2006). Influence of EPIYA-repeat polymorphism on the phosphorylation-dependent biological activity of Helicobacter pylori CagA. Gastroenterology *130*, 1181-1190.

Nelson, W. J. (2008). Regulation of cell-cell adhesion by the cadherin-catenin complex. Biochem Soc Trans *36*, 149-155.

Nelson, W. J., and Nusse, R. (2004). Convergence of Wnt, beta-catenin, and cadherin pathways. Science *303*, 1483-1487.

Nelson, W. J., Shore, E. M., Wang, A. Z., and Hammerton, R. W. (1990). Identification of a membrane-cytoskeletal complex containing the cell adhesion molecule uvomorulin (E-cadherin), ankyrin, and fodrin in Madin-Darby canine kidney epithelial cells. J Cell Biol *110*, 349-357.

Odenbreit, S., Puls, J., Sedlmaier, B., Gerland, E., Fischer, W., and Haas, R. (2000). Translocation of Helicobacter pylori CagA into gastric epithelial cells by type IV secretion. Science *287*, 1497-1500.

Ohnishi, N., Yuasa, H., Tanaka, S., Sawa, H., Miura, M., Matsui, A., Higashi, H., Musashi, M., Iwabuchi, K., Suzuki, M.*, et al.* (2008). Transgenic expression of Helicobacter pylori CagA induces gastrointestinal and hematopoietic neoplasms in mouse. Proc Natl Acad Sci USA *105*, 1003-1008.

Pollack, A.L., Barth, A.I., Altschuler, Y., Nelson, W.J. and Mostov, K.E., (1997). Dynamics of beta-catenin interactions with APC protein regulate epithelial tubulogenesis. J Cell Biol 137, 1651-62

Poppe, M., Feller, S. M., Römer, G., and Wessler, S. (2007). Phosphorylation of Helicobacter pylori CagA by c-Abl leads to cell motility. Oncogene *26*, 3462-3472.

Pounder, R. E., and Ng, D. (1995). The prevalence of Helicobacter pylori infection in different countries. Aliment Pharmacol Ther *9 Suppl 2*, 33-39.

Ren, S., Higashi, H., Lu, H., Azuma, T., and Hatakeyama, M. (2006). Structural basis and functional consequence of Helicobacter pylori CagA multimerization in cells. Journal of Biological Chemistry *281*, 32344.

Saadat, I., Higashi, H., Obuse, C., Umeda, M., Murata-Kamiya, N., Saito, Y., Lu, H., Ohnishi, N., Azuma, T., Suzuki, A.*, et al.* (2007). Helicobacter pylori CagA targets PAR1/MARK kinase to disrupt epithelial cell polarity. Nature *447*, 330-333.

Selbach, M., Moese, S., Hauck, C. R., Meyer, T. F., and Backert, S. (2002). Src is the kinase of the Helicobacter pylori CagA protein *in vitro* and *in vivo*. J Biol Chem *277*, 6775-6778.

Stein, M., Bagnoli, F., Halenbeck, R., Rappuoli, R., Fantl, W. J., and Covacci, A. (2002). c-Src/Lyn kinases activate Helicobacter pylori CagA through tyrosine phosphorylation of the EPIYA motifs. Mol Microbiol *43*, 971-980.

Stewart, A., Ham, C., and Zachary, I. (2002). The focal adhesion kinase amino-terminal domain localises to nuclei and intercellular junctions in HEK 293 and MDCK cells independently of tyrosine 397 and the carboxy-terminal domain. Biochem Biophys Res Commun *299*, 62-73.

Suzuki, M., Mimuro, H., Kiga, K., Fukumatsu, M., Ishijima, N., Morikawa, H., Nagai, S., Koyasu, S., Gilman, R. H., Kersulyte, D.*, et al.* (2009). Helicobacter pylori CagA phosphorylation-independent function in epithelial proliferation and inflammation. Cell host & microbe *5*, 23-34.

Suzuki, M., Mimuro, H., Suzuki, T., Park, M., Yamamoto, T., and Sasakawa, C. (2005). Interaction of CagA with Crk plays an important role in Helicobacter pylori-induced loss of gastric epithelial cell adhesion. J Exp Med *202*, 1235-1247.

Tammer, I., Brandt, S., Hartig, R., König, W., and Backert, S. (2007). Activation of Abl by Helicobacterpylori: A Novel Kinase for CagA and Crucial Mediator of Host Cell Scattering. Gastroenterology *132*, 1309-1319.

Tan, S., Tompkins, L. S., and Amieva, M. R. (2009). Helicobacter pylori usurps cell polarity to turn the cell surface into a replicative niche. PLoS pathogens *5*, e1000407.

O'Toole P.W., Lane, M.C. and Porwollik S. (2000). Helicobacter pylori motility. Microbes Infect 2 (10) pp. 1207-14

Uemura, N., Okamoto, S., Yamamoto, S., Matsumura, N., Yamaguchi, S., Yamakido, M., Taniyama, K., Sasaki, N., and Schlemper, R. J. (2001). Helicobacter pylori infection and the development of gastric cancer. NEJM *345*, 784-789.

Vogelmann, R., Amieva, M. R., Falkow, S. and Nelson, W. J., (2004). Breaking into the epithelial apical-junctional complex--news from pathogen hackers. Curr. Opin. Cell Biol. 16, 86-93

Vogelmann, R., and Nelson, W. J. (2005). Fractionation of the epithelial apical junctional complex: reassessment of protein distributions in different substructures. Mol Biol Cell *16*, 701-716.

Wessler, S., and Backert, S. (2008). Molecular mechanisms of epithelial-barrier disruption by Helicobacter pylori. Trends Microbiol *16*, 397-405.

Wiedemann, T., Loell, E., Mueller, S., Stoeckelhuber, M., Stolte, M., Haas, R., and Rieder, G. (2009). Helicobacter pylori cag-Pathogenicity island-dependent early immunological response triggers later precancerous gastric changes in Mongolian gerbils. PLoS ONE *4*, e4754.

Yamada, S., and Nelson, W. J. (2007). Localized zones of Rho and Rac activities drive initiation and expansion of epithelial cell-cell adhesion. J Cell Biol *178*, 517-527.

Yokozaki H., (2000). Molecular characteristics of eight gastric cancer cell lines established in Japan. Pathol Int 50, 767-777.

Zeaiter, Z., Cohen, D., Musch, A., Bagnoli, F., Covacci, A., and Stein, M. (2007). Analysis of detergent-resistant membranes of Helicobacter pylori infected gastric adenocarcinoma cells reveals a role for MARK2/Par1b in CagA-mediated disruption of cellular polarity. Cell Microbiol *10*, 781-794.

7 Acknowledgements

First of all I would like to thank Dr. Roger Vogelmann for giving me this very interesting project, for the continuous support and the always very interesting and fruitful discussions.

I would also like to thank Prof. Dr. Michael Schemann for supporting my doctoral thesis at the Center of Life and Food Sciences Weihenstephan

Prof. Dr. Roland Schmid I would like to thank for giving me the opportunity to work at the 2nd Dept. of Internal Medicine, Klinikum rechts der Isar, Munich.

I am very grateful to my group Victoria Doll, Katrin Maier, Claudia Weiss and Fabian Coscia for continuous support with the many projects, for helpful discussions and all the good times. I would also like to thank the people from the different groups especially Annegret Schmidt, Emina Savarese, Mariel Paul and Sandra Baumann.

Many thanks go to Manuel R. Amieva for providing the G27 CagA wt plasmid and anti-CagA-NT antibody, W. James Nelson for providing MDCK cells and plasmids for the TCF/β-catenin transcription assay, Elke Burgermeister for NCI-N87 gastric cells, Markus Gerhard for help with the TCF/β-catenin transcription assay. Special thanks go to Benjamin Balluff for help with statistics.

Special thanks go to the members of the Dept. of Microbiology, Klinikum rechts der Isar, Munich, Germany for their technical support with confocal microscopy especially Susi Dürr and Frank Schmitz.

Finally and most importantly, I would like to thank my husband Christian Pelz and my family for constantly supporting me in the best way I could possibly imagine.